GLOBAL BIOGEOCHEMICAL CYCLES, VOL. 20, GB3018, doi:10.1029/2004GB002407, 2006

C:N stoichiometry of the biological pump in the North Atlantic: Constraints from climatological data

W. Koeve[1,2,3]

Received 9 November 2004; revised 28 February 2006; accepted 21 March 2006; published 7 September 2006.

[1] Recently and independently published estimates of global net community production which were based on seasonal changes of either nutrients (NO_3 and PO_4 (Louanchi and Najjar, 2000)) and salinity normalized dissolved inorganic carbon (NC_t (Lee, 2001)) in the surface ocean indicate that the stoichiometry of new production strongly differs from the well-established remineralization ratios in the deep ocean (the Redfield ratio). This difference appears to be most pronounced in the North Atlantic Ocean. Data quality issues as well as methodological differences in the data analysis applied in the published studies, however, make this comparison of nutrient- and carbon-based estimates ambiguous. Here I present an analysis based on a combination of historical data (World Ocean Atlas and Data 1998) and empirical approaches and provide a reassessment of the C:N elemental ratio of new (export) production in the North Atlantic. It is found that the estimate of winter nutrient fields is the most crucial step in estimating basin-scale, time-integrated C:N ratios of new production. An approach is developed which allows an estimate of winter nitrate and total CO_2 concentrations which are consistent with estimates from an isopycnal outcrop analysis where these are available. Regional trends in the spring + summer integrated C:N ratio of new production suggest an increase from high latitudes toward the subtropics. The basin-integrated C:N ratio of new production between 40°N and 65°N is 11.4 ± 1.4, far exceeding the Redfield ratio. The bulk C_{org}:C_{inorg} rain ratio estimated for the same region is 7.7. The fate of organic carbon produced in excess of the Redfield equivalent of nitrate uptake is discussed. It is suggested that a considerable fraction of excess carbon is remineralized above the depth of the winter mixed layer.

Citation: Koeve, W. (2006), C:N stoichiometry of the biological pump in the North Atlantic: Constraints from climatological data, *Global Biogeochem. Cycles*, *20*, GB3018, doi:10.1029/2004GB002407.

1. Introduction

[2] The biological pump [*Volk and Hoffert*, 1985] drives a net flux of fixed organic carbon from the surface of the ocean into its interior. This flux, and the subsequent remineralization in the deep ocean produces a vertical gradient of total CO_2, which controls the steady state CO_2 level of the atmosphere [*Shaffer*, 1993]. To determine the effectiveness of this carbon flux is at the heart of carbon cycle studies in the ocean [*Scientific Committee on Oceanic Research*, 1990; *Fasham et al.*, 2001]. Net community production (NCP), which is the excess of phytoplankton primary production over community respiration, is an important measure of the strength of the biological pump, in particular if, on appropriate time and space scales, it can be equated with the export of organic matter ("export production") from the euphotic zone [*Dugdale and Goering*, 1967; *Eppley and Peterson*, 1979]. Over seasonal to annual timescales, net community production may be estimated from the mass balance of nutrients, oxygen or CO_2 [*Jenkins and Goldman*, 1985; *Minas and Codispoti*, 1993; *Emerson et al.*, 1993, 1997] between late winter and the end of the growth season.

[3] Recently, global net community production has been estimated from seasonal changes of phosphate and nitrate [*Louanchi and Najjar*, 2000], salinity normalized total dissolved inorganic carbon [*Lee*, 2001] and the oxygen flux across the air-sea interface [*Najjar and Keeling*, 2000]. Global NCP estimates (all conversions are based on standard Redfield elemental ratios C:N:P = 106:16:1) ranged between 4.6 and 8.0 GT C yr^{-1}, where global NCP estimates based on either carbon or oxygen data [*Najjar and Keeling*, 2000; *Lee*, 2001] provide the high-end estimates (6.7 to 8.0 GT C yr^{-1}) while nutrient-based estimates [*Louanchi and Najjar*, 2000] suggest lower NCP (4.6 to 5.3 GT C yr^{-1}). Hence differences between C (O_2) and N (P) based estimates could reflect global mean elemental ratios of NCP in excess of the Redfield

[1]Zentrum für Marine Umweltwissenschaften (MARUM), University of Bremen, Bremen, Germany.
[2]Also at Laboratoire d'Etudes en Géophysique et Océanographie Spatiales, Observatoire Midi Pyrénées, Toulouse, France.
[3]Now at Leibniz-Institut für Meereswissenschaften (IFM-GEOMAR), Kiel, Germany.

0886-6236/06/2004GB002407

Table 1a. Apparent C:N:P Ratio of Net Community Production Estimated From Published Estimates: Global Estimates, C:N = 8.0 – 11.4. C:P = 112 – 160

Method	Source	C, Tmole C yr^{-1}	O_2, Tmole C yr^{-1}	N, Tmole N yr^{-1}	P, Tmole P yr^{-1}
NCP_{ML} (NC_t)	*Lee* [2001]	560[a]			
NCP_{ML} (A_t + pCO_{2sw})	*Lee* [2001]	670[a]			
Oxygen air-sea flux + seasonal storage analysis	*Najjar and Keeling* [2000]		470–560[b]		
Seasonal amplitude of nutrient change[c]	*Louanchi and Najjar* [2000]			59	4.2

[a]I use data of *Lee* [2001, Table 1], which are not scaled up by the correction factor which he suggests to account for NCP during the cooling season (see also the discussion in section 3.5.3). *Lee* [2001] presents two independent estimates of NCP in the mixed layer: NCP_{ML} (NC_t) uses salinity normalized total CO_2 data which are computed from empirical relationships between temperature, nitrate and NC_t; NCP_{ML} (A_t + pCO_{2sw}) uses NC_t data which are computed from alkalinity and pCO_2. (For details see also section 2.4.)

[b]Conversion to carbon assumes a -O_2:C ratio of 1.45.

[c]NCP estimates from the analysis of nutrient data represent seasonal changes, integrated over 100 m depth, during spring and summer [*Louanchi and Najjar*, 2000].

stoichiometry [*Koeve and Ducklow*, 2001]. The magnitude of the problem is summarized in Tables 1a and 1b. Global mean C:N ratios between 8.0 and 11.4 and C:P ratios between 112 and 160 emerge from this interpretation. Though such values are within the range of elevated C:N ratios which have been observed in individual studies [*Sambrotto et al.*, 1993a; *Kähler and Koeve*, 2001; *Körtzinger et al.*, 2001a], global mean C:N values of that magnitude are difficult to reconcile with mean elemental ratios of remineralization in the interior of the ocean which have been estimated to range between 6.4 and 7.7 [*Redfield et al.*, 1963; *Takahashi et al.*, 1985; *Anderson and Sarmiento*, 1994; *Shaffer*, 1996; *Körtzinger et al.*, 2001b]. Some of the difference between apparent C:N ratios of new production (i.e., $\Delta NC_t^*/\Delta NO_3$-ratios; computed from seasonal changes of nitrate, ΔNO_3, and total dissolved inorganic carbon, ΔNC_t, and including corrections for air sea gas exchange of CO_2 and particulate inorganic carbo production, hence ΔNC_t^*) and C:N ratios of remineralization may be explained by N_2-fixation, however, current high end-estimates of global open ocean N_2-fixation (100 Tg N yr^{-1} [*Codispoti*, 1997]) are about a factor of 2 to 6 lower than the N_2-fixation required to explain the apparent global C:N ratios from Tables 1a and 1b (i.e., 190 to 640 Tg N).

[4] A closer look to the Atlantic Ocean, where most of the evidence for elevated C:N ratios of new production comes from [*Sambrotto et al.*, 1993a; *Bates et al.*, 1996; *Daly et al.*, 1999; *Körtzinger et al.*, 2001a; *Koeve*, 2004], shows apparent C:P uptake ratios of 157 to 202 (Table 1b) which is about a factor of 2 larger than recently estimated deep water remineralization ratios of 73–80 [*Li and Peng*, 2002]. Breaking down the C:P ratios of NCP into latitude bands (trophic regions) suggests that the major source region for elevated apparent stoichiometric ratios is in the high latitudes, in particular the North Atlantic "bloom regions," rather than the low latitudes where one might expect N_2-fixation to be important [*Gruber and Sarmiento*, 1997]. The aim of this paper is to provide a detailed re-evaluation of the $\Delta NC_t^*/\Delta NO_3$ ratio of NCP in the temperate and subarctic North Atlantic from a climatological viewpoint.

2. Material and Methods

[5] NCP estimates are calculated in this study based on the seasonal difference between winter and summer data sets of nitrate or salinity normalized total dissolved inorganic carbon (NC_t), representing data from just before and

Table 1b. Apparent C:N:P Ratio of Net Community Production Estimated From Published Estimates: Atlantic Ocean

Region	Latitude	NCP_{ML} (NC_t) From *Lee* [2001], Tmole C yr^{-1}	NCP_{ML} (A_t + pCO_{2sw}) From *Lee* [2001], Tmole C yr^{-1}	O_2-Analysis From *Najjar and Keeling* [2000], Tmole C yr^{-1}	PO_4 From *Louanchi and Najjar* [2000], Tmole P yr^{-1}	C: P, mole:mole
Temperate and subarctic North Atlantic	40°N–70°N	53	59	66	0.17	312–388
Subtropical and tropical Atlantic	40°S–40°N	51	49	71–82[a]	0.42	117–195
Southern Ocean (Atlantic sector)	south of 40°S	59	81	63	0.45	131–180
Atlantic Ocean		163[b]	189[b]	200–210[c]	1.04	157–202

[a]NCP estimates from the analysis of nutrient data represent seasonal changes, integrated over 100 m depth, during spring and summer [*Louanchi and Najjar*, 2000].

[b]I use data of *Lee* [2001, Table 1], which are not scaled up by the correction factor which he suggests to account for NCP during the cooling season (see also the discussion in section 3.5.3). *Lee* [2001] presents two independent estimates of NCP in the mixed layer: NCP_{ML} (NC_t) uses salinity normalized total CO_2 data which are computed from empirical relationships between temperature, nitrate and NC_t; NCP_{ML} (A_t + pCO_{2sw}) uses NC_t data which are computed from alkalinity and pCO_2. (For details see also section 2.4.)

[c]The first value is, as reported by *Louanchi and Najjar* [2000, Table 3], for the extratropical Atlantic Ocean only. The second value is computed by adding an estimate for the tropical Atlantic based on *Louanchi and Najjar*'s [2000] phosphate based NCP estimate being in Redfield proportion (C:P = 106).

Table 2a. Acronyms and Data Sets: Data Sets Computed in This Study

Acronym	Element or Property	Remark
Nutrient data sets		
LN_summer	N	means of July–August–September (for Northern Hemisphere summer) of the monthly resolved nutrient data set prepared by *Louanchi and Najjar* [2000]
LN_minimum	N	annual minimum in the monthly nutrient data set of *Louanchi and Najjar* [2000]
WOA_summer	N	WOA98 summer data set (usually July–August–September in the Northern Hemisphere)
WOA_minimum	N	annual minimum in the 3-monthly nutrient analyzed data set of WOA 1998
LN_winter	N	means of January–February–March (for Northern Hemisphere winter) of the *Louanchi and Najjar* [2000] nutrient data set
LN_maximum	N	annual maximum in the monthly nutrient data set of *Louanchi and Najjar* [2000]
WOA_winter	N	January–February–March climatology (Northern Hemisphere winter) from the seasonal WOA98 data set
GBexWOA (vd, pt, pd)	N	winter nutrient distribution calculated by applying the extrapolation method of *Glover and Brewer* [1988] to the annual WOA98 analyzed nutrient data field; for the standard case the mixed layer depth is estimated from the variable density criterion (vd); sensitivity computations are done with mixed layer depth estimates using constant temperature (pt) and constant density criteria (pd)
KexWOA (vd, pt, pd)	N	winter nutrient distribution based on GBexWOA and a correction for the spring-summer nutrient remineralization as estimated from the AOU on the winter mixed layer depth plane and an AOU/NO_3 conversion factor
KKKM		winter nutrient estimates from an isopycnal outcrop analysis [*Körtzinger et al.*, 2001a]
Carbon data sets		
TA	alkalinity	monthly data set of total alkalinity at the sea surface, computed from monthly T and S (WOA98) using empirical formulae from *Millero et al.* [1998]
Alk × pCO_2	C	monthly data set of salinity (WOA98) normalized total dissolved inorganic carbon, computed from TA and monthly pCO_2
Winter subset		the winter time slice is defined as the NC_t value from the month of the deepest mixing
Summer subset		the summer time slice is defined as the annual minimum NC_t value
GBexLee	C	winter NC_t calculated with the 'T × NO_3' algorithms of *Lee et al.* [2000] from GBexWOA nitrate data and temperature data from the month of deepest mixing interpolated to $Z = Z_{max}$
KexLee	C	like NC_t-GBexLee but with KexWOA nitrate data
KexLeeSST	C	like NC_t-KexLee but with SST data from the month of deepest mixing
LNwLee	C	winter NC_t calculated with the "T × NO_3" algorithms from LN-winter nitrate data and temperature data from the respective 3-monthly WOA98 temperature climatology (usually January–February–March in the North Atlantic)
LNsLee	C	like NC_t-LN-winter, but with LN-summer nitrate data and respective temperature data (in the North Atlantic usually July–August–September)
WOAwLee	C	winter NC_t calculated with the "T × NO_3" algorithms from WOA_winter nitrate and temperature data (usually January–February–March in the North Atlantic)
WOAsLee	C	summer NC_t calculated with the "T × NO_3" algorithms from WOA_summer nitrate and temperature data (in the North Atlantic usually July–August–September)
Seasonal differences		
KexWOAmin	N	KexWOAvd – WOA_minimum
	C	KexLeeSST – WOAsLee
GBexWOAmin	N	GBexWOAvd – WOA_minimum
	C	GBexLee – WOAsLee
LN_based	N	LN_winter – LN_summer
	C	LNwLee – LNsLee

Table 2b. Acronyms and Data Sets: External Data Sets

Acronym	Property	Remarks
WOA98 (annual climatology)	T, S, NO_3, AOU, oxygen saturation	annual climatology, global data set, 3D, 1° × 1° http://www.nodc.noaa.gov
WOA98 (seasonal/3-montly climatology)	T, S, NO_3	seasonal climatology, global data set, 3D, 1° × 1° http://www.nodc.noaa.gov
WOA98 (monthly climatology)	T, S	monthly climatology, global data set, 3D, 1° × 1° http://www.nodc.noaa.gov; [*Conkright et al.*, 1998]
LN	NO_3	monthly climatology, global data set, 3D (upper 500 m), 2° × 2° http://www1.whoi.edu/jgofs.html *Louanchi and Najjar* [2000]
pCO_2 air-sea difference	ΔpCO_2	monthly climatology, global data set, 2D (surface), 4° × 5° [*Takahashi et al.*, 1999; T. Takahashi, personal communication, 2000]
wind speed	u, v	monthly climatology, global data set, 2D, surface, 4° × 5° http://ingrid.ldgo.columbia.edu/SOURCES/.OSUSFC/.DATA/.wspd/ [*Esbensen and Kushnir*, 1981]
wind speed	u, v	monthly climatology, computed for the time period 1960–2001 http://iridl.ldeo.columbia.edu/SOURCES/.NOAA/.NCEP-NCAR/.CDAS-1/

at the end of the phytoplankton growth season. Several independent nitrate and NC_t data sets are constructed for both time slices (Table 2a; see the next two sections for details). Sources of publicly available data sets used in this study are given in Tables 2b and 2c. In particular, I make use of the monthly nitrate climatology of *Louanchi and Najjar* [2000] and nitrate, oxygen, temperature and salinity climatologies of variable temporal resolution from the NODC World Ocean Atlas 1998 (WOA98) [*Conkright et al.*, 1998; *Antonov et al.*, 1998; *Boyer et al.*, 1999]. Calculations are performed for the North Atlantic between the equator and 65°N. Marginal seas (Baltic See, Hudson Bay, North Sea, Mediterranean) are excluded. Where necessary, data are regridded to the NODC standard vertical grid (0, 10, 20, 30, 50, 75, 100, 125, 200, 250, 300, 400, 500 m) and to a 1° × 1° horizontal grid.

2.1. Nitrate Data Sets

2.1.1. Summer

[6] The nitrate data set "LN_summer" is estimated according to *Louanchi and Najjar* [2000] as the mean of July–August–September from the monthly resolving nitrate climatology of *Louanchi and Najjar* [2000]. The nitrate data set "LN_minimum" is estimated as the local annual minimum in the same climatology. The nitrate data set "WOA_minimum" is constructed as the local annual minimum in the seasonal (winter, spring, summer, autumn) WOA98 data set [*Conkright et al.*, 1998].

2.1.2. Winter

[7] There are no winter nitrate data from the central open ocean North Atlantic between 35°N–40°N and 65°N (55°W to 1°W) available from the WOA98, the WOA 2001, or the eWOCE archive (Electronic Atlas of WOCE Data, Version 2, June 2000 [*Schlitzer*, 2000]) (see section 3.1). All published estimates for the winter season from this region are therefore based on interpolations in space [*Conkright et al.*, 1998], space and time [*Louanchi and Najjar*, 2000] or extrapolated from the vertical nutrient distribution in spring and summer [*Glover and Brewer*, 1988; *Koeve*, 2001]. In this study the following estimates will be used. The nitrate data set "LN_winter" is calculated as the mean of January–February–March (Northern Hemisphere winter) of the monthly LN data set [*Louanchi and Najjar*, 2000]. "LN_maximum" is the local annual nitrate maximum in that monthly data set; this maximum is usually observed in February or March in the North Atlantic. The nitrate data set "WOA_winter" is the January–February–March time slice of the seasonal WOA98 data set and the data set "WOA_maximum" is the local annual nitrate maximum of the seasonal WOA98 data set (see Table 2a for details).

[8] Several other nitrate data sets are constructed adopting methods which extrapolate winter data fields from the vertical nitrate distribution observed during summer or spring and which are discussed in more detail by *Glover and Brewer* [1988] and *Koeve* [2001]. The "extrapolation technique" of *Glover and Brewer* [1988] predicts the winter nutrient concentration from summer or spring nitrate concentration observed at the depth of maximum wintertime mixing. The theory behind this is that the rapid shallowing of the mixed layer in spring [*Monterey and Levitus*, 1997] leaves behind a depth layer between the seasonal thermocline and the permanent thermocline which, to the first order, preserves its wintertime properties over spring and summer. In this model seasonal remineralization is regarded

Table 2c. Acronyms and Data Sets: Other Acronyms

Acronym	Remark
NCP	net carbon production
WOA	World Ocean Atlas (gridded data; climatologies); available from the NODC
WOD	World Ocean Database (non-gridded, station data); available from the NODC
eWOCE	Electronic Atlas of WOCE Data, Version 2 (June/2000), [*Schlitzer*, 2000]

as not being significant at the depth plane of the maximum winter mixed layer. In the study of *Glover and Brewer* [1988] summer nutrient observations from the TTO-NAS program [*Brewer et al.*, 1985] were combined with winter mixed layer depth estimates based on 3-monthly resolved temperature and salinity climatologies [*Levitus*, 1982]. Here I apply the extrapolation method to objectively analyzed data ($1^\circ \times 1^\circ$ resolution) from the WOA98 (Table 2b). As nutrient data set I use the annual nitrate climatology from WOA98; where most of the data in the temperate and subarctic open ocean North Atlantic are from spring, summer and autumn. The winter mixed layer depth estimate is based on the monthly temperature and salinity climatologies from WOA98 and computed as follows. A variable density criterion [*Levitus*, 1982; *Monterey and Levitus*, 1997], which estimates the mixed layer depth by interpolating to the depth at which the potential density equals the density of a water mass which has the properties of (SST $-$ 0.5°C) and the surface salinity, is used as the standard case. The winter mixed layer depth is the annual maximum of the mixed layer depth. Sensitivity calculations are carried out with mixed layer depth data sets for which either a constant change in potential temperature (SST $-$ 0.5°C), or a constant change in potential density (sea surface density 0.125) are used. All three winter mixed layer data sets are combined individually with the annual nitrate climatology from WOA98 and the winter nitrate concentration is estimated as the uncorrected local nitrate concentration on the depth plane of the winter mixed layer depth data set. This gives three independent winter nitrate data sets, "GBexWOAvd" (standard case), "GBexWOApt" and "GBexWOApd" (Table 2a).

[9] The extrapolation approach tends to overestimate winter nutrient concentrations, when the effect of shallow remineralization during spring and summer is not corrected for [*Koeve*, 2001]. Using information from oxygen saturation data, this shortcoming can be reduced significantly [*Koeve*, 2001]. Ignoring the effect of lateral advection in the first instance one can calculate the preformed nitrate concentration, $NO_{3(pref)}$, from equation (1) [*Emerson and Hayward*, 1995]. Here $NO_{3(obs)}$ is the observed nitrate concentration, AOU is the apparent oxygen utilization and R is the molar ratio of oxygen consumed:nitrate released during remineralization and all properties are concentrations on the winter mixed layer depth plane.

$$NO_{3(pref)} = NO_{3(obs)} + AOU/R. \quad (1)$$

[10] Estimates of R on shallow isopycnals just below the permanent thermocline in the North Atlantic range between -8.6 and -9.4 [*Takahashi et al.*, 1985; *Minster and Boulahdid*, 1987; *Li and Peng*, 2002]. The complete oxidation of organic matter of marine origin requires oxygen in a O_2:N ratio of -9.05 [*Hedges et al.*, 2002] to -9.3 [*Anderson*, 1995]. I choose a value of R = -9.1 [*Minster and Boulahdid*, 1987]. AOU and oxygen saturation (O_{2s}) are taken from the annual climatology of the WOA98 and estimated for the depth plane of the winter mixed layer depth via the extrapolation technique. Throughout this paper I will refer to the AOU corrected winter nitrate estimates from WOA98 data to as the data set "KexWOA"; again the standard computation (KexWOAvd) applies the variable density criterion for the mixed layer depth estimate and sensitivity computations are carried out with pt and pd mixed layer data sets.

[11] Another, completely independent, set of winter nitrate estimates is based on an isopycnal outcrop analysis of data from a N-S transect along 20°W. For this method a linear regression of nitrate concentration and oxygen concentration for a given isopycnal is computed and the outcrop nitrate concentration is estimated as the crossing point with the 98% oxygen saturation isoline. The geographical assignment of the outcrop of a given isopycnal is based on a comparison of outcrop temperatures and winter minimum temperatures estimated from remote sensing observations. Such an analysis has recently be carried out for nitrate and total CO_2 for the northeast Atlantic by *Körtzinger et al.* [2001a]. Standard errors of nitrate outcrop values were equivalent to about 7.5% of the outcrop concentration and usually lower than 0.5 μmole kg^{-1} (for details, see *Körtzinger et al.* [2001a, Table 3 and Figures 5 and 6]). The a priori choice of the winter time oxygen saturation of 98% is based on small-scale studies from the Biotrans NABE site (47°N, 20°W) and an evaluation of climatological data. The mean oxygen saturation of remnant winter water in the Biotrans NABE region was 97.8(±0.7)% [*Koeve*, 2001]. Using regression slopes of oxygen saturation vs. nitrate concentrations of -2.2 to -2.5 (% / μmole * kg) from the same study, the uncertainty of outcrop nitrate concentrations related to the uncertainty of the oxygen saturation state can be quantified to be about 0.3 μmole kg^{-1}. The area-weighted mean of the climatological winter oxygen saturation data at the oceans surface (WOA 98, January–March) between 40°N and 65°N is 97.9%; the standard error of this estimate is about 0.1%. It is important to note here that the isopycnal outcrop analysis does not apply any a priori correction of nutrient remineralization to the observed nitrate data on the isopycnals. Hence that method is completely independent of any explicit assumption concerning the AOU/R remineralization ratio used elsewhere in this study. I will use the outcrop analysis based winter nitrate data set together with estimates of nitrate concentrations from early spring during the NABE (North Atlantic Bloom Experiment [*Ducklow and Harris*, 1993]) and a detailed study of winter nitrate concentrations at the NABE-47°N site [*Koeve*, 2001] as a benchmark for the other estimates.

2.2. NC_t From A_t and $pCO_{2\ (sea)}$

[12] Basically following a method suggested by *Millero et al.* [1998] and described in detail by *Lee* [2001] a monthly resolved data set of salinity normalized total dissolved inorganic carbon, NC_t, of the surface mixed layer is estimated from the distribution of alkalinity (A_t) and surface ocean pCO_2 (in the following referred to as the 'Alk × pCO_2-method'). Here a monthly data set of total alkalinity is calculated from climatological temperature and salinity surface data from WOA98 and empirical relationships proposed by *Millero et al.* [1998]. Surface ocean pCO_2 is estimated from sea-air difference (ΔpCO_2 [*Takahashi et al.*,

1999]) and atmospheric pCO_2 data [*Masarie and Tans*, 1995]. Assuming that gradients in atmospheric pCO_2 over the Atlantic are primarily north-south, a monthly resolved $1° \times 1°$ atmospheric pCO_2 data set is constructed from 16 island-based or coastal air sampling stations in the Atlantic Ocean. Air-sea difference data ($4° \times 5°$ grid resolution) are regridded to the standard $1° \times 1°$ grid used in this study. Total dissolved inorganic carbon (C_t), is calculated from total alkalinity, A_t, and $pCO_{2(sea)}$ using the software package of *Lewis and Wallace* [1998]. The carbonic acid dissociation constants after *Mehrbach et al.* [1973] as refitted by *Dickson and Millero* [1987], which gave highest consistency when DIC was calculated from A_t and fCO_2 or pCO_2 [*Lee et al.*, 1997; *Körtzinger et al.*, 2001a], are applied. NC_t is calculated as the dissolved inorganic carbon concentration normalized to a salinity of 35 using the formula $NC_t = C_t * 35/S$, where S is taken from the monthly WOA98 climatology.

2.3. NC_t From SST and Nitrate Data

[13] *Lee et al.* [2000] proposed a set of regionalized empirical relationships between NC_t, nitrate and sea surface temperature (in the following referred to as the "$T \times NO_3$-approach"). This approach is applied to several of the above-mentioned nitrate data sets from summer and winter. Temperature data sets are extracted from WOA98 to match the nitrate data sets with respect to timing and depth. The $T \times NO_3$ approach is applied to data from the upper 100 m. For the winter time slice an idealized constant vertical distribution of NC_t within the upper 100 m is assumed; for the summer time slice the vertical profile is resolved.

2.4. Analysis

[14] One major obstacle to the direct comparison of data presented by *Louanchi and Najjar* [2000] and *Lee* [2001] lies in their differing approaches to perform the temporal and vertical integration of NCP. *Louanchi and Najjar* [2000] integrated the seasonal difference (LN_winter − LN_summer) of 3-monthly means of their monthly climatology over the upper 100 m. No estimate of diffusion from below this layer was included. NCP was calculated from seasonal nutrient deficits by conversion with standard elemental ratios (C:P = 106 [*Redfield et al.*, 1963]). *Lee* [2001] computed NCP for the mixed layer only, however, allowing for seasonal changes (monthly to 3-monthly) of the depth of this layer. That study also included an estimate of diffusive carbon fluxes from below the mixed layer, and an estimate of CO_2 air-sea exchange.

[15] During summer the mixed layer depth in the temperate and subpolar North Atlantic is much smaller than the euphotic zone or the nitrate impoverished depth layer. From the WOA98 summer temperature data set, for example, a mean mixed layer depth (depth at which T = SST-0.5) of about 23 m is found for the open ocean North Atlantic between 40°N and 65°N. In the nitrate seasonal difference data set of *Louanchi and Najjar* [2000] the mean depth at which the difference (LN_winter − LN_summer) becomes zero is 81 ± 16 m. Partly the nitrate deficit below the summer mixed layer may be because of convective mixing events early in the growth season [*Koeve*, 2001; *Koeve et al.*, 2002]. In addition, subsurface nitrate uptake by phytoplankton proceeds throughout the growth season in the depth layer of the subsurface chlorophyll *a* maximum. In the North Atlantic the depth of this subsurface chl-a maximum and the associated nitracline increases with a mean rate of about 10 m/month over the growth season [*Strass and Woods*, 1988, 1991]. Hence estimating NCP from the mixed layer only must be an underestimate of the annual euphotic zone NCP.

[16] Combining the approaches of *Louanchi and Najjar* [2000] and *Lee* [2001], however, is not straightforward. In particular the computation of NC_t from A_t and pCO_2 is restricted to the surface mixed layer since no subsurface pCO_2 data fields are available. The NC_t estimation from empirical relationships with SST and nitrate, however, may be extended to waters below the surface mixed layer by replacing SST with a vertical profile of the in situ temperature.

[17] The approach which I use here is as follows. First, seasonal changes (winter - summer values) of nitrate and NC_t (from the "$T \times NO_3$-approach") are estimated as a 3-D data field. Vertical integration is performed within the upper 100 m as long as the seasonal difference is positive (equations (2) and (3)). Net production of organic carbon (ΔOC) is computed from ΔNC_t, the CO_2 air-sea exchange (ASE) and an estimate of the production of particulate inorganic carbon, referred here to as ΔIC (equation (4)).

$$\Delta NO_3 = \int_{Z=0}^{Z=\min\left(100, Z_{NO_{3w}=NO_{3s}}\right)} (NO_{3w} - NO_{3s}), \qquad (2)$$

$$\Delta NC_t = \int_{z=0}^{Z=\min\left(100, Z_{NC_{tw}=NC_{ts}}\right)} (NC_{tw} - NC_{ts}), \qquad (3)$$

$$\Delta OC = \Delta NC_t + ASE - \Delta IC. \qquad (4)$$

[18] Air-sea exchange (ASE) is integrated between February and August, the months which typically represent the time of deepest winter mixing in the climatology and the time of summer nitrate minimum. The monthly air-sea exchange is calculated from monthly pCO_2 sea-air-difference data from the *Takahashi et al.* [1999] data set according to equation (5). The solubility of CO_2 in seawater, K_H, was calculated after *Weiss* [1974]. *Sc* is the Schmidt number of CO_2, calculated according to *Wanninkhof* [1992]. For the wind speed dependence of the transfer velocity *k*, the parameterization after *Wanninkhof* [1992] for climatological winds (equation (6a)) is used as the standard case. Formulations suggested by *Wanninkhof and McGillis* [1999] (equation (6b)), *Nightingale et al.* [2000] (equation (6c)) and *Liss and Merlivat* [1986] (equation (6d)) are used in sensitivity calculations. Here u_{av} is the climatological wind speed average (in $m \cdot s^{-1}$) at 10 m above sea level. Climatological wind speed data for this calculation were taken from the *Esbensen and Kushnir* [1981] data set (standard runs) and from a 41-year climatology of wind speeds from the NCEP reanalysis [*Kalnay et al.*, 1996]. Temperature and

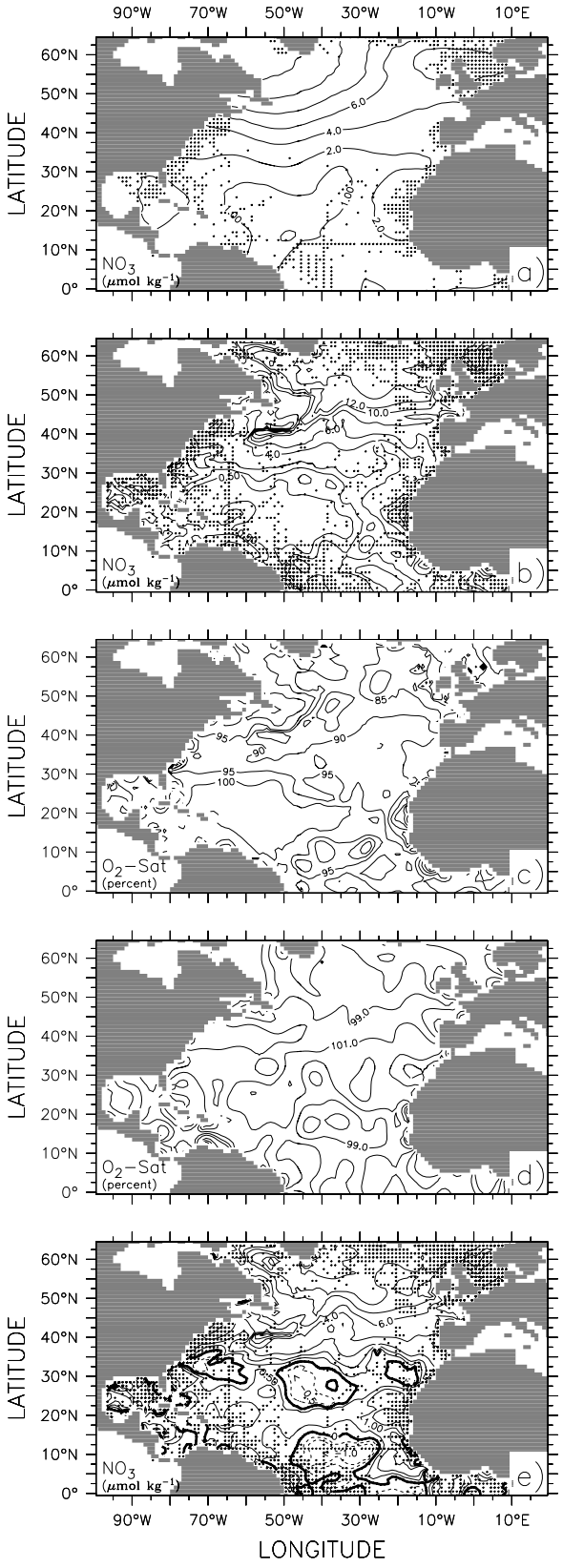

salinity data from the monthly WOA98 database are taken for computing Sc (Tables 2a and 2b).

$$F = k \cdot \left(\frac{Sc}{660}\right)^{-1/2} \cdot K_H \cdot \Delta pCO_2, \tag{5}$$

$$k = 0.39 \cdot u_{av}^2, \tag{6a}$$

$$k = 1.09 \cdot u_{av} - 0.333 \cdot u_{av}^2 + 0.078 \cdot u_{av}^3, \tag{6b}$$

$$k = 0.333 \cdot u_{av} + 0.222 \cdot u_{av}^2, \tag{6c}$$

$$\begin{aligned} k &= 0.17 \cdot u_{av} && (u_{av} < 3.6\,m/s). \\ k &= 2.85 \cdot u_{av} - 9.65 && (3.6\,m/s < u_{av} < 13\,m/s) \\ k &= 5.9 \cdot u_{av} - 49.3 && (u_{av} < 13\,m/s) \end{aligned} \tag{6d}$$

[19] The estimate of particulate calcium carbonate production (ΔIC) is based on the concept of potential alkalinity [*Fiadeiro*, 1980; *Robertson et al.*, 1994] and computed from seasonal changes of salinity normalized alkalinity (NA_t) and nitrate (equation (7)). A monthly resolving data set of NA_t is

Figure 1. Estimates of the winter nitrate distribution. (a) LN_winter: Winter surface nitrate distribution estimated as the seasonal mean for January, February, and March of the monthly resolving nitrate data set of *Louanchi and Najjar* [2000]. Diamonds indicate the grid points for which historical data are available for this time period (WOA unanalyzed data). (b) Winter nitrate data field estimated by applying the extrapolation method of *Glover and Brewer* [1988] to the annual mean nitrate data set from the WOA98 (for details see the text). Diamonds indicate the grid points for which historical data are available in the unanalyzed annual nitrate composite of WOA98. (c) Oxygen saturation on the winter mixed layer depth plane. The extrapolation method is applied to the annual oxygen saturation data set of WOA98. (d) Oxygen saturation at the sea surface during Northern Hemisphere winter, extracted from the seasonal data set of the WOA98. The data distribution of the unanalyzed oxygen data set is not shown, however, unlike for nitrate winter data (see Figure 1a); oxygen data are available for about 50% of the grid points between 30°N and 65°N, with a very good representation of the open ocean. Data distribution plots are available from the NODC website http://www.nodc.noaa.gov/OC5/WOA98F/woaf_cd/search.html. (e) Winter nitrate data field estimated after correcting the estimates shown in Figure 1b by the nitrate equivalent of the seasonal apparent oxygen utilization (AOU) on the depth plane of the winter mixed layer depth. The AOU data set is from the annual WOA98 climatology. Like in Figure 1b, diamonds indicate the grid points for which historical data are available in the unanalyzed annual nitrate composite of WOA98.

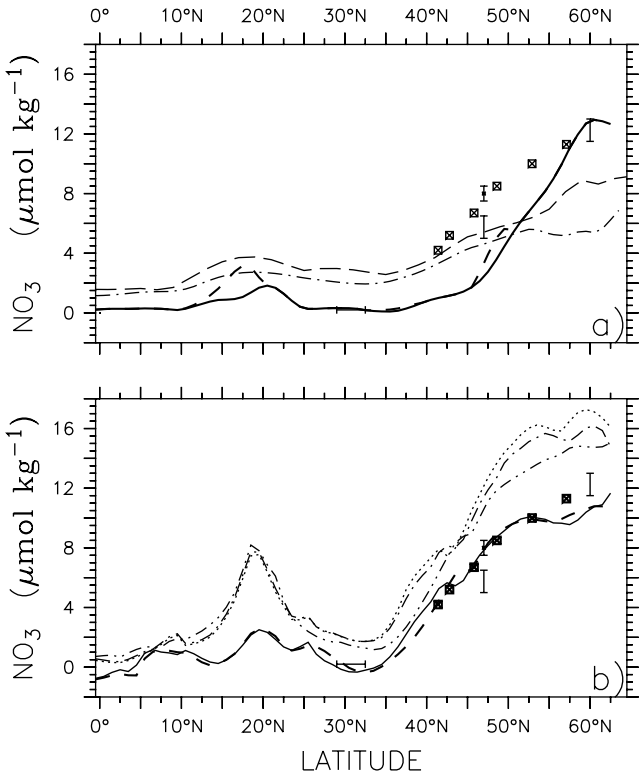

Figure 2. A comparison of the distribution of different surface nitrate estimates along 20°W during winter. For acronyms, see Tables 2a, 2b, and 2c. (a) Estimates from published climatologies: LN_winter (thin dash-dotted line), LN_maximum (thin dashed line), WOA_winter (thick solid line), and WOA-maximum (thick dashed line). (b) Winter estimates from summer to winter extrapolation techniques. GBexWOAvd (thin dash-dotted line), GBexWOApd (thin dotted line), GBexWOApt (thin dash-dot-dotted line), KexWOAvd (thick solid line), KexWOA98pt (thick dashed line). In both plots, bars indicate ranges of observations from JGOFS process studies during early spring: 59°N–60°N, upper range (~13 μmole kg^{-1}) from R/V *Atlantis* cruise 119/4 during late April 1989 and lower range (10.5 μmole kg^{-1}) from FS *Meteor* cruise 10/2 during late May 1989; 47°N, ~ 6 μmole kg^{-1} from R/V *Atlantis* cruise 119/4 during late April 1989 and 5.0 to 6.5 μmole kg^{-1} from FS *Meteor* cruise 21/1 during late March 1992. All data are from U.S. and German JGOFS data archives. Squares indicate winter nitrate estimates from the isopycnal outcrop analysis [*Körtzinger et al.*, 2001a]. The standard error of the latter ranged between 0.3 and 0.7 μmole kg^{-1}. Star with vertical bar at 47°N refers to estimates from the "O_2-step" method discussed by *Koeve* [2001]; the vertical bar gives the range of interannual variation estimated for that site.

calculated from WOA98 temperature data according to *Millero et al.* [1998]. Since the NA_t-T relationship of Millero et al. is formally described for the mixed layer only, a mixed layer value, ΔIC_{ML}, is calculated from mixed layer ΔNA_t and ΔNO_3 data first. The ΔOC:ΔIC- ratio of the mixed layer (or the "rain ratio" of the surface mixed layer, RR_{ML}; equation (8)) is then computed using a concomitant mixed layer estimate of ΔOC_{ML} (units μmole kg^{-1}) which is computed like in equation (4)) from $\Delta NC_{t\text{-}ML}$, a mixed layer depth corrected estimate of ASE (basically ASE/Z_{ML}) and ΔIC_{ML} (units μmole kg^{-1}). Assuming that ΔOC: ΔIC in the upper 100 m is constant to the first order, the surface ocean integral value of ΔIC is estimated from $\Delta OC/RR_{ML}$ (equation (9)). Finally, the C:N ratio of net community production is estimated from equation (10).

$$\Delta IC_{ML} = (\Delta NA_t + \Delta NO_3)/2, \tag{7}$$

$$RR_{ML} = {}^{\Delta OC_{ML}}\Big/_{\Delta IC_{ML}}, \tag{8}$$

$$\Delta OC = (\Delta NC_t + ASE)/(1 + 1/RR_{ML}), \tag{9}$$

$$(C:N)_{NCP} = \frac{\Delta OC}{\Delta NO_3}. \tag{10}$$

3. Results and Discussion

3.1. Winter Nitrate Distribution

[20] Winter nitrate concentrations vary widely between the various methods used in this study (Figures 1a, 1b, 1e, 2a, and 2b). In the temperate northeast Atlantic (50°N–60°N), for example, minimum and maximum estimates differ by more than 10 μmole kg^{-1} or a factor of 3 to 4 (Figures 2a and 2b). Generally the data sets which are based on interpolations in space (WOA_winter, WOA_maximum, LN_winter, LN_maximum) show much lower concentrations in the temperate and subarctic North Atlantic compared with data sets which are based on summer to winter extrapolation techniques (GBexWOA, KexWOA). At 50°N, for example, the LN_winter data set shows winter nitrate concentrations between about 5 μmole kg^{-1} at 20°W and 10 μmole kg^{-1} at 50°W (Figure 1a). At the same latitude the winter nitrate distribution based on the extrapolation method of *Glover and Brewer* [1988] (GBexWOAvd) shows concentrations around 15 μmole kg^{-1} over most of the basin (Figure 1b). One major caveat of all attempts to describe the winter nitrate distribution from regional interpolation of winter time observations is the scarcity of data during that season. In Figure 1a, diamonds indicate grid cells for which data are available for the time period January to March. (WOA 2001 was checked for winter nitrate data, too, and showed a small number of additional grid cells with winter data around Ireland, but no additional data in the open ocean.) It becomes clear from this that the N-S distribution of winter nitrate in WOA_winter and hence the predicted location of the nutrient front between oligotrophic and nutrient replete waters builds on the interpolation of observations from close to Iceland in the north, stations at about 30°N in the south, and stations close to the continents in the east and west. The method of *Louanchi and Najjar* [2000] to construct monthly nutrient data sets

includes temporal data interpolation, and combines 1-monthly, 3-monthly and 5-monthly composites. If winter time observations are rare, like in the North Atlantic, this approach interpolates winter data from autumn and spring observations and hence, since a maximum can not be found from interpolation, will underestimate winter time concentrations in temperate and subpolar waters (data set LN_minimum in Figure 2a). Estimating the winter nitrate distribution in the Northern Hemisphere as the mean of January–February–March [*Louanchi and Najjar*, 2000] further smoothes the distribution (LN_winter in Figure 2a). The comparison with NABE data (shown as bars in Figure 2a), estimates from the outcrop analysis (squares in Figure 2a) and the winter nitrate estimates from 47°N/20°W [*Koeve*, 2001] indicates that, at least in the northeast Atlantic, winter estimates based on WOA98 data or the *Louanchi and Najjar* [2000] data set underestimate the winter time concentrations in temperate and subarctic waters. It is noteworthy, though not in the focus of this study, that the *Louanchi and Najjar* [2000] data appear to overestimate winter concentrations in the subtropics and hence most likely overestimate NCP there. Winter nitrate estimates based on the extrapolation technique (GBexWOA, Figure 2b) are subject to a number of systematic problems, like the influence of seasonal remineralization on winter nitrate estimates [*Koeve*, 2001] and the choice of the winter mixed layer criterion, which require attention.

[21] The shallowing of the mixed layer in spring is a rapid process [*Monterey and Levitus*, 1997] which leaves the depth layer between the seasonal and the permanent thermoclines secluded from air-sea exchange at the surface of the ocean. Under these conditions remineralization of organic matter leads to a seasonal oxygen debt (apparent oxygen utilization, AOU) which can be used to estimate the size of the seasonal nitrate release between winter and summer [*Koeve*, 2001]. The magnitude of this problem is evident from the distribution of the oxygen saturation on the depth plane of the winter mixed layer (Figure 1c) which shows oxygen saturation below 90% in large areas north of about 40°N. This is much less compared with the "observed" winter time (March) oxygen saturation in the surface mixed layer of the WOA98 climatology, which is close to 100% saturation (Figure 1d). Owing to mixing with deep waters impoverished of oxygen and despite the effect of bubble injection [*Craig and Hayward*, 1987], a value of about 98% saturation appears to be more typical for winter condition in the deep mixing regimes of temperate and subarctic North Atlantic [*Koeve*, 2001] (Figure 1d). The area-weighted mean of the climatological winter oxygen saturation data at the oceans surface (WOA 98, January–March) between 40°N and 65°N is 97.9%; the standard error of this estimate is about 0.1%.

[22] The preformed nitrate concentration, $NO_{3(pref)}$, is estimated as described in section 2 (see equation (1)). I use two estimates of the seasonal AOU at the depth of the winter mixed layer plane. The first is extrapolated from the annual WOA98 AOU data set and assumes $O_{2Sat\ (pref)}$ = 100%. The second is recalculated from this AOU and the accompanying O_{2Sat} data set and assumes a winter time oxygen saturation of $O_{2Ssat\ (pref)}$ = 98%.

[23] The estimated distribution of $NO_{3(pref)}$ (KexWOA, Figure 1e) shows consistently lower winter time nitrate values compared with the GBexWOA data set (Figure 1b), but still much higher values compared with LN_winter (Figure 1a). Estimated $NO_{3(pref)}$ concentrations at the NABE-47 station (47°N, 20°W) are 7.5 to 8.1 μmole kg^{-1} and compare well with results from a recent detailed local study (7.8 ± 0.8 μmole kg^{-1} [*Koeve*, 2001]) which was based on independent data and methods. For the section along 20°W (Figure 2b) the comparison with the estimates based on the isopycnal outcrop analysis, taken from *Körtzinger et al.* [2001a], shows that KexWOA tracks the position of the nitrate front the best among all data sets. The only exception is a moderate underestimate of winter nitrate concentrations in KexWOA in the very north.

[24] In subtropical regions, KexWOA usually predicts winter nitrate concentrations close to zero. Occasionally, however, negative preformed nitrate values are predicted at the northern and southern boundaries of the subtropical gyre (Figure 1e). This is a reminiscent of similar features observed in the subtropical North Pacific [*Emerson and Hayward*, 1995] and indicative that the remineralization of low-nitrogen dissolved organic matter [*Kähler and Koeve*, 2001] which can significantly contribute to oxygen consumption on shallow isopycnals below the subtropical gyre of the Pacific and Indian Ocean [*Doval and Hansell*, 2000; *Abell et al.*, 2000] and thereby increases the AOU:NO_3 ratio of remineralization (R in equation (1)). On deep isopycnals, which crop out in temperate and subarctic waters, however, the contribution of DOM remineralization to AOU was insignificant in the Pacific and Indian Ocean [*Doval and Hansell*, 2000]. Furthermore, regions of negative $NO_{3(pref)}$ reduce in size if an $O_{2S(pref)}$ = 98% is assumed. By analogy with the findings of *Doval and Hansell* [2000] and backed up by the very good agreement between KexWOA and the winter estimates from the isopycnal outcrop analysis (Figure 2b), it is therefore concluded that the value of R = −9.1 is a reasonable choice for temperate and subarctic waters.

[25] Estimates of winter nitrate concentrations from the extrapolation method are sensitive to the choice of the mixed layer criterion. Along 20°W, for example, differences of up to a few micromoles between pt and pd based estimates are seen (GBexWOA estimates in Figure 2b). Fortunately, most of this sensitivity disappears after correction for seasonal remineralization [*Koeve*, 2001] (KexWOA estimates in Figure 2b). From this I estimate the uncertainty of the KexWOA winter nitrate estimate to be better than ±0.5 μmole kg^{-1}.

3.2. Winter NC_t Distribution

[26] Winter NC_t along 20°W, calculated from T × NO_3- and Alk × pCO_2-algorithms, are shown in Figure 3. In high latitudes the range between the maximum and minimum estimates is about 50 μmole kg^{-1}, which is the same magnitude as the seasonal NC_t change in this region (*Takahashi et al.* [1993] and this study; see below). Minimum and maximum estimates are from NC_t computed with the T × NO_3 approach from the LN_winter and GBexWOA nitrate estimates, respectively. The accompanying winter temperature data sets (not shown) differ by about 0.5°C

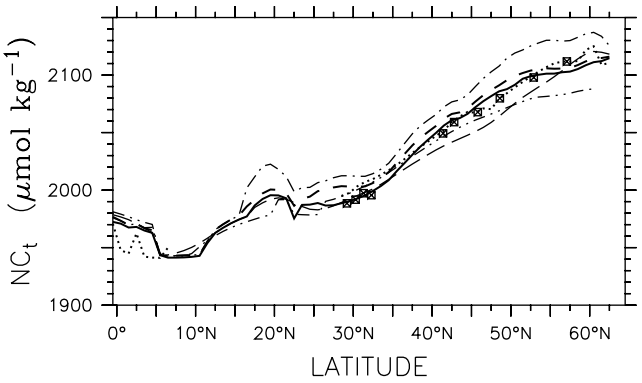

Figure 3. Salinity normalized total dissolved inorganic carbon (NC_t) in the surface mixed layer during winter along 20°W in the North Atlantic (for acronyms, see text and Table 2a): KexLeeSST (thick solid line), KexLee (thick dashed line), Alk × pCO_2 (thick dotted line), GBexLee (thin dash-dotted line), WOAwLee (thin long dashed line), and LNwLee (thin dash-dot-dotted line). For comparison, estimates from an isopycnal outcrop analysis (squares north of 40°N) and winter time observations (squares south of 40°N) from *Körtzinger et al.* [2001a] are shown.

since LN_winter (and WOA_winter) use SST while GBexWOA uses the winter temperature on the Z_{max} depth plane, which by definition of the mixed layer criterion is 0.5°C lower than the SST. For the section along 20°W (north of 30°N) this temperature difference corresponds to a difference in NC_t of about 4–5 μmole kg^{-1}. This is equivalent to 10–20% of the overall difference between LN_winter and GBexWOA based estimates. Hence the major source of the uncertainty in winter NC_t estimates from T × NO_3 algorithms is due to the uncertainty in winter nitrate estimates.

[27] Moderate NC_t values are found for the KexWOA based estimate (data set "KexLee") and the Alk × pCO_2 based estimate. Along 20°W the latter agree with the estimates from the isopycnal outcrop analysis [*Körtzinger et al.*, 2001a] within a few μmole kg^{-1}. In fact, most of the difference between KexLee and Alk × pCO_2 is now due to the corresponding differences in temperature. KexLee utilizes the winter temperature on the Z_{max} depth plane while the surface mixed layer alkalinity, which is used to estimate the Alk × pCO_2 based NC_t data set, implies sea surface temperature (SST). The corresponding difference in NC_t of 4–5 μmole kg^{-1} is about the size and direction of the difference between KexLee and Alk × pCO_2. I conclude that, as for winter nitrate, reconciling estimates from KexLee, Alk × pCO_2 and the isopycnal outcrop method allow an estimate of the most likely winter NC_t distribution in the temperate and subarctic North Atlantic. If the winter nitrate estimates from KexWOA are combined with winter SST a NC_t distribution (data set "KexLeeSST") is computed which compares even better with the NC_t from the Alk × pCO_2 approach (Figure 4) and the isopycnal outcrop analysis. For both data sets, winter NC_t increases from values around 1940 to 1960 μmole kg^{-1} in the subtropical gyre to values larger than 2100 μmole kg^{-1} north of 50°N. The mean difference (RMS) between both estimates is about 6 μmole kg^{-1}.

3.3. Summer Nitrate and NC_t Distribution

[28] Owing to nitrate uptake during the phytoplankton spring bloom, most of the North Atlantic is nitrate depleted (NO_3 < 0.5 μmole kg^{-1}) in the surface mixed layer at the end of summer [*Strass and Woods*, 1991; *Yentsch*, 1990; *Campbell and Aarup*, 1992]. For waters south of Iceland, however, several authors [e.g., *Veldhuis et al.*, 1993; *Sambrotto et al.*, 1993b] report nitrate concentrations of several micromoles that persist over the growth season. All summer nitrate data sets (Table 2a) analyzed in this study reproduce this north-south distribution (Figure 5a). Differences between data sets are small (<2 μmole kg^{-1}) compared with differences in winter nitrate estimates discussed above. Owing to the interpolation procedures applied [*Louanchi and Najjar*, 2000], gradients in the data set LN_summer are smooth. Along 20°W surface nitrate concentrations in this data set increase from slightly below 1 μmole kg^{-1} in subtropical waters toward about 2.5 μmole kg^{-1} south of Greenland. The data set WOA_minimum shows a stronger gradient between lower nitrate concentrations in the subtropics and concentrations around 4 μmole kg^{-1} around 60°N. A nutrient front is observed between 50°N and 55°N. An analysis of data compiled in the eWOCE archive (2nd edition [*Schlitzer*, 2000]; data not shown) supports the latter picture of a strong nitrate front at about 50°N–55°N. Surface summer data from south of this

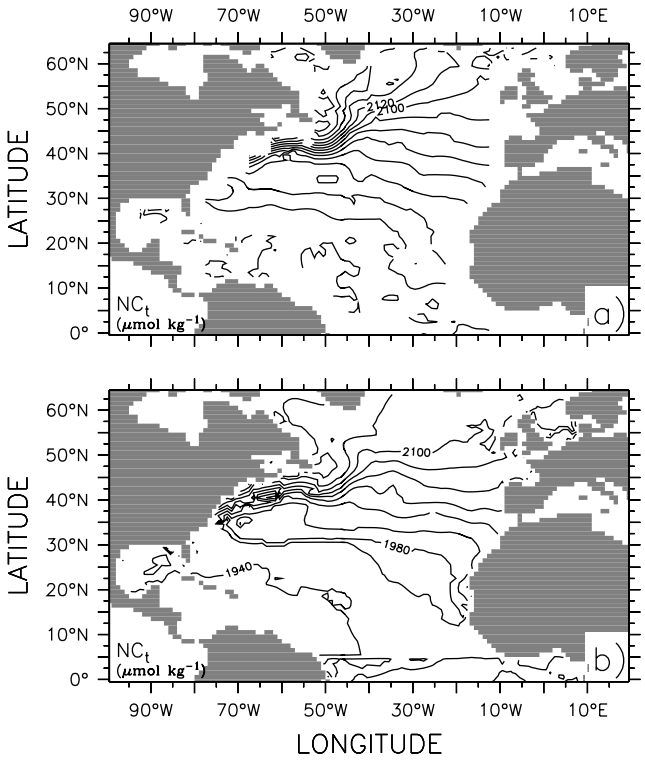

Figure 4. Salinity normalized total dissolved inorganic carbon (NC_t) in the surface mixed layer during winter in the North Atlantic Ocean. (a) Alk × pCO_2. (b) KexLeeSST.

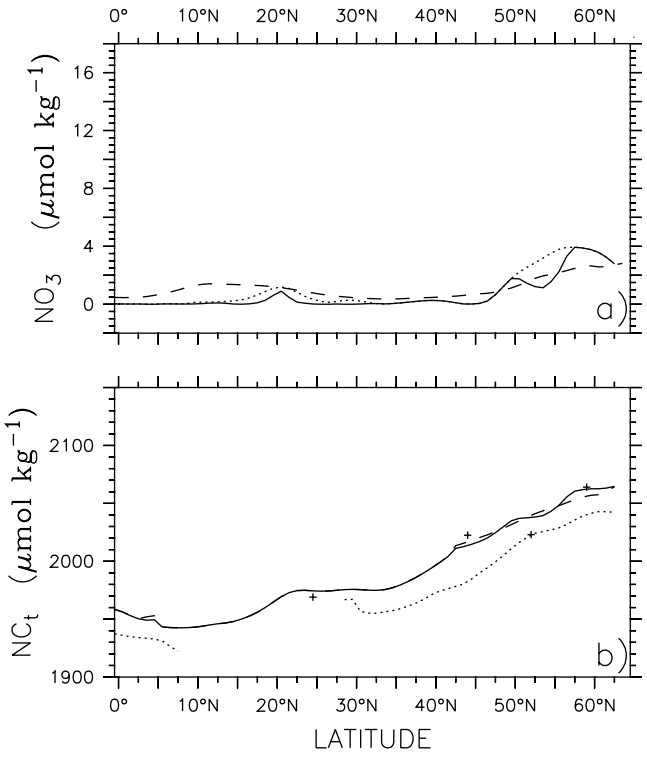

Figure 5. Distribution of nitrate and salinity normalized total dissolved inorganic carbon in the surface mixed layer during summer along 20°W in the North Atlantic. (a) Summer nitrate distribution: WOA_minimum (solid line), WOA_summer (dotted line), and LN_summer (dashed line). (b) Summer NC_t estimates: WOAsLee (solid line), LNsLee (dashed line), and Alk × pCO_2 (dotted line).

latitude are essentially zero, concentrations north of this front are around 5 μmole kg^{-1}. Still, with the combined data from the WOCE program and the historical data from the WOA98, the subarctic North Atlantic is undersampled during the narrow time slot between the end of the summer phytoplankton bloom and the renewed cooling. The exact distribution of the minimum summer nitrate concentration in the subarctic North Atlantic remains vague. Whether, and why, nitrate uptake appears to stop at a concentration of about 4 to 5 μmole kg^{-1} needs further work.

[29] Differences in summer nitrate estimates propagate into very small differences when summer NC_t is computed from the T × NO_3 approach (Figure 5b). However, the Alk × pCO_2 approach suggest annual minimum NC_t along 20°W which are 13 ± 12 μmole kg^{-1} lower in the North Atlantic. From total-CO_2 data compiled in the eWOCE archive, three east-west sections cross the 20°W longitude during summer (plus signs in Figure 5b). Two crossing-overs at 44°N and 59°N show NC_t surface values of 2021 to 2024 μmole kg^{-1} and 2062 to 2066 μmole kg^{-1}, respectively, which are very close to the T × NO_3 based estimates. These stations where sampled in June (1997, WOCE section A24). The respective surface nitrate concentrations are 0 to 0.5 μmole kg^{-1} and 4.8 to 5 μmole kg^{-1}. Another WOCE line (A05, sampled late July), crossed the 20°W line at 24.5°N and had a NC_t value of 1969 μmole kg^{-1}. A third section intersects at about 52°N and was sampled during September (1991, WOCE section A01E) and has a NC_t concentration of 2023 μmole kg^{-1}, which is very close to the annual minimum of the Alk × pCO_2 based estimate of NC_t. Unfortunately, only few stations from this late season section have total CO_2 data from the surface mixed layer. They are always in between T × NO_3 and Alk × pCO_2 based NC_t summer estimates from nearby grid points. This brief analysis suggests that ΔNC_t estimates which use summer NC_t data from the T × NO_3 approach might be slight underestimates. However, since Alk × pCO_2 based estimates are only available from the surface mixed layer and due to the uncertainty how to extrapolate this surface difference over depth, I regard the summer NC_t estimates from the T × NO_3 approach the most reasonable summer data set which can be used during this study.

Table 3. Integrated Nitrate and Carbon Budgets (Σ0–100 m) of the Temperate and Subarctic North Atlantic (40°N to 65°N)[a]

Estimate	NO_3 Budget, mole N m^{-2}	OC-NC_t Budget, mole C m^{-2}	ΔNCt_{seas}, mole C m^{-2}	ASE, mole C m^{-2}	IC Prod., mole C m^{-2}	C:N, mole:mole
KexWOAmin						
EC-W92 (std)[b]	0.29	3.3	2.4	1.3	0.43	11.3
NCEP-41-W92[c]				1.5		12.2
NCEP-41-WM99[d]				1.8		13.2
NCEP-41-LM86[e]				0.8		9.7
NCEP-41-N00[f]				1.0		10.8
LN_based[g]	0.22	2.8		1.3		12.6
GBexWOAmin[h]	0.59	4.0		1.3		6.9

[a]Data sets which are used to compute the N and C seasonal differences for KexWOAmin, GBexWOAmin, and LN_based are given in Table 2a (seasonal differences).

[b]For KexWOAmin, ASE is estimated using the wind speed climatology of *Esbensen and Kushnir* [1981] and using the formulation of the wind speed dependence of the CO_2 exchange coefficient, k, for long-term averaged winds of *Wanninkhof* [1992].

[c]ASE is from 41-year climatology of the NCEP reanalysis data [*Kalnay et al.*, 1996] and *Wanninkhof* [1992] wind speed dependence of k.

[d]ASE is from NCEP-41 winds and the *Wanninkhof and McGillis* [1999] wind speed dependence of k.

[e]ASE is from NCEP-41 winds and the *Liss and Merlivat* [1986] formulation of the wind speed dependence of k.

[f]ASE is from NCEP-41 winds and the *Nightingale et al.* [2000] formulation of the wind speed dependence of k.

[g]For LN_based, ASE is from of *Esbensen and Kushnir* [1981] climatological winds and the *Wanninkhof* [1992] wind speed dependence of k.

[h]For GBexWOAmin, ASE is as for LN_based.

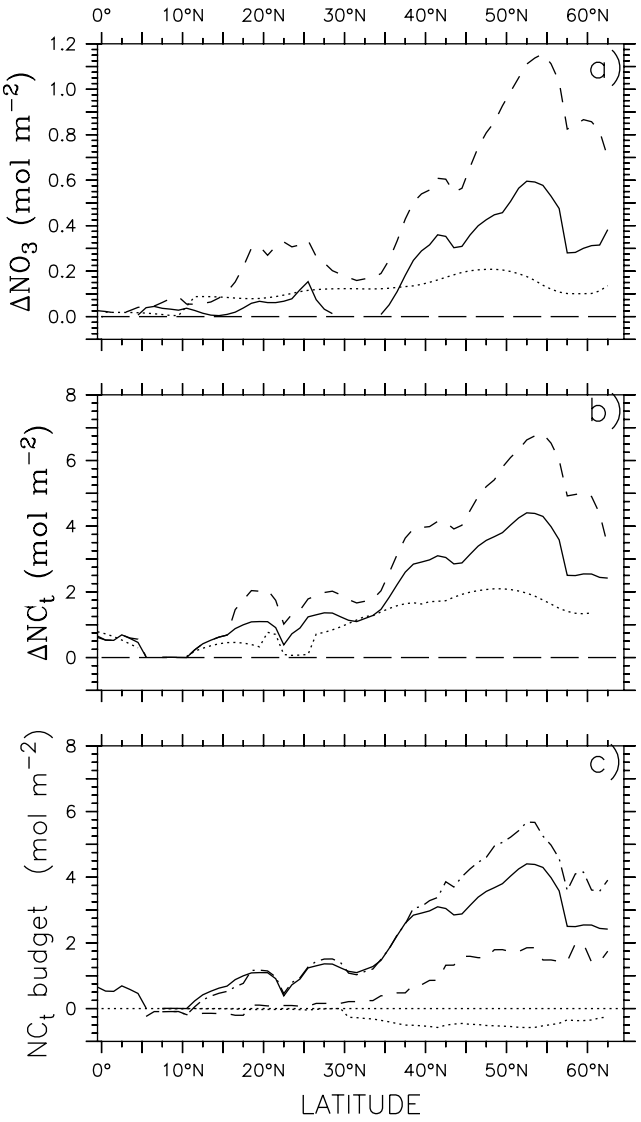

Figure 6. Nitrate and total CO_2 uptake along 20°W, integrated over the upper 100 m. (a) Seasonal nitrate uptake: KexWOAmin (solid line), GBexWOAmin (dashed line), and LN-based (dotted line). (b) Seasonal change of NC_t (symbols like in Figure 6a). (c) NC_t-budget of KexWOAmin. Seasonal NC_t-change (ΔNC_t; dash-dotted line), air-sea exchange (ASE; dashed line), $CaCO_3$ production (given as negative values, $-\Delta IC$, to indicate that $CaCO_3$ production has to be subtracted from the seasonal NC_t change; dotted line) and net production of organic carbon (ΔOC; solid line), computed according to equation (4), are shown. For acronyms, see Table 2a (seasonal differences).

3.4. Seasonal Nutrient and Carbon Budget

[30] From the larger number of winter and summer nitrate and NC_t data sets a subset of three winter-summer pairs is chosen for further analysis (Tables 2a (seasonal differences) and 3). These represent high-end winter concentration estimates (GBexWOAmin), low-end winter estimates (LN_based) and one based on the AOU corrected winter nitrate data (KexWOAmin).

[31] Both ΔNO_3 and ΔNC_t (Figures 6a and 6b) increase northward along 20°W and show maxima between 47°N (LN_based) and 55°N (GBexWOAmin). Large differences, however, exist for the magnitude of the three ΔNO_3 and ΔNC_t estimates shown, for example, the maxima along 20°W range from 0.2 mole NO_3 m^{-2} (LN_based) to 1.15 mole NO_3 m^{-2} (GBexWOAmin) and 2.2 mole NC_t m^{-2} (LN_based) to 6.9 mole NC_t m^{-2} (GBexWOAmin), respectively. Additional variation is added through the contribution of ASE and ΔIC to the carbon budget. For KexWOAmin, which is shown as an example (Figure 6c), CO_2 air-sea gas exchange can add up to 50% to the observed ΔNC_t. The relative importance of ASE for the carbon budget differs between data sets. It is largest for LN and lowest for GBexWOAmin. Production of $CaCO_3$ on the other hand (Figure 6c) usually accounts for about 10% to 20% of the total carbon uptake. Estimates of this fraction and the ΔOC: ΔIC 'rain ratio' show only little variations between data sets but consistent regional patterns with an increase toward the north along 20°W (Figure 7).

[32] Not surprisingly, estimates of the C:N ratio from the three data sets are very different, too (Figure 8). For the LN data set an increase toward the north is predicted, C:N ratios along 20°W range from about 8 at 30°N to about 28 at 60°N. GBexWOAmin and KexWOAmin suggest increasing C:N ratios toward the oligotrophic subtropical North Atlantic. GBexWOAmin predicts a moderate increase from about 6.6 at 60°N to about 10 at 30°N. KexWOAmin varies between about 10 and 14 north of 37°N and rapidly increased south of 37°N. For the North Atlantic between 40°N and 65°N (260°E–380°E), mean annually integrated C:N ratios of 6.9 (GBexWOAmin), 11.3 (KexWOAmin) and 12.6 (LN_based) are estimated.

3.5. Limitations and Uncertainties

3.5.1. Error Estimates

[33] A two-fold range (6.9 to 12.6) of the mean annual C:N ratio of new production in the temperate and subarctic

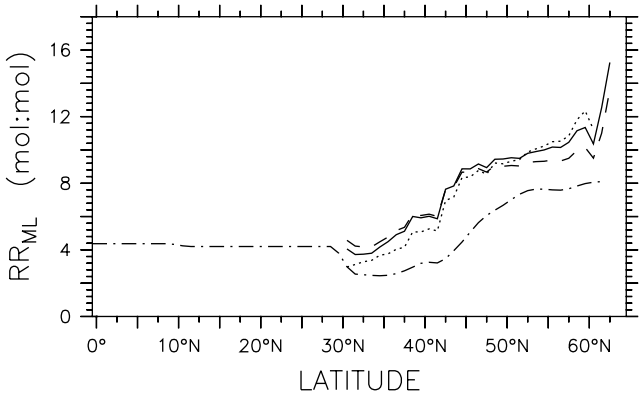

Figure 7. Ratio of organic carbon to inorganic carbon uptake in the mixed layer along 20°W: KexWOAmin (solid line), GBexWOAmin (dashed line), and LN-based (dotted line). Dash-dotted line is an estimate of RR_{ml} [from *Koeve et al.*, 2002] which assumes a constant C:N ratio (6.6) and winter and summer nitrate distribution similar to KexWOAmin.

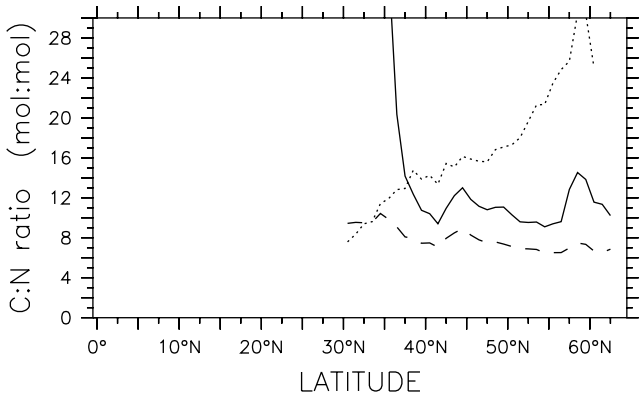

Figure 8. C:N uptake ratio along 20°W, estimated from integrals (upper 100 m) of the seasonal NC_t budget (see Figure 6c) and nitrate uptake (see Figure 6a): KexWOAmin (solid line), GBexWOAmin (dashed line), and LN-based (dotted line).

North Atlantic between 40°N and 65°N is found from the above data analysis. This range is in particular due to differences in the winter nitrate (and NC_t) estimates (Figures 1–4). From the current analysis the KexWOAmin estimate appears to be the most reliable one since its estimates of winter nitrate and NC_t are backed up by data from the isopycnal outcrop analysis of *Körtzinger et al.* [2001a] (Figures 2 and 3), spring and winter time observations in the northeast Atlantic [*Koeve*, 2001] and the congruence of estimate from $pCO_2 \times$ Alk and $T \times NO_3$ based estimates of NC_t (Figure 3). A statistical error estimate for the C:N ratio of NCP of KexWOAmin is given in Appendix A. Of more significance are systematic uncertainties, for example, regarding the magnitude of CO_2 air-sea exchange and its effect on the C:N estimate (Table 3). Using a suite of different formulations of the wind speed dependence of gas exchange (see section 2.4), C:N ratios of NCP between 9.7 and 13.2 are found for the integral of KexWOAmin, with a mean value (± standard deviation) of 11.4 (±1.4). Also, the OC:IC ratio of carbon export is currently under discussion. For the temperate/subarctic North Atlantic recent estimates range from 4.3–6.1 [*Koeve*, 2002], 5.3–5.9 [*Lee*, 2001], 7.7 (this study) and >40 [*Sarmiento et al.*, 2002]. Assuming that the OC:IC ratio is either half or 5 times its estimated value (7.7) reflects the range of recently proposed OC:IC values and yields C:N ratios of NCP ranging between 9.9 and 12.6, similar to the uncertainty range derived from different CO_2 air-sea exchange algorithms.

3.5.2. Vertical Diffusion and Advection, Horizontal Advection

[34] Estimating the contribution of vertical diffusion to the carbon and nitrate budgets and the C:N ratio of NCP requires that the temporal development of the NO_3 and NC_t gradients in the upper 100 to 200 m can be quantified. Given the sparse data distribution during winter and spring this is not possible and hence, the effect of vertical diffusion is ignored in this study. I regard this a minor problem, according to the following arguments. In the nutrient-replete temperate and subarctic North Atlantic the seasonal change in nitrate concentrations is about 1 order of magnitude larger compared to oligotrophic waters [*Lipschultz et al.*, 2002], for which *Ono et al.* [2001] concluded a significant impact of vertical diffusion on estimates of stoichiometric ratios. *Lee* [2001] estimated that vertical diffusion contributed about 3% to their carbon budget between 40°N and 70°N in the Atlantic. Furthermore, the ratio of NC_t and NO_3 fluxes due to vertical diffusion should largely scale according to the C:N uptake ratios itself [*Sambrotto et al.*, 1993a], since the uptake ratio largely defines the vertical gradients of NC_t and NO_3 below the mixed layer. For the same reasons, I assume that vertical advection has little impact on the estimates of the C:N uptake ratio. Horizontal advection can be a significant component of the local nitrate or NC_t budget at a given grid point. For example, *Oschlies et al.* [2000] estimated that on an annual basis the horizontal transport within the upper 126 m was equivalent to 25% of the vertical mixing flux of nitrate into this layer at the NABE-47°N site. In order to evaluate the effect of horizontal advection on seasonal uptake rates, winter time temperature observations were compared with extrapolated winter time temperatures (details not shown). The latter were computed in analogy to the extrapolated winter nitrate data field (see section 2.1). In the northeast Atlantic, for example, extrapolated temperatures are about 1°C too cold compared with winter time observations at the surface. This is equivalent to a mean N-S transport of about 2° latitude over the growth season. Correspondingly both the seasonal nitrate and NC_t concentration differences are somewhat too large (for example at 45°N by <1 μmole NO_3 kg^{-1} and <10 μmole NC_t kg^{-1}). This uncertainty in winter nutrient concentrations is equivalent to about 15% of the seasonal nutrient drawdown (ΔNO_3, ΔNC_t). The slope ratio of winter NC_t and nitrate is about 10 between 35°N and 55°N. Propagating this effect through the computation of the C:N ratio of NCP is not straightforward. However, given the size of this effect, the similarity of the winter time NC_t to nitrate slope ratio with the regional mean of the overall C:N ratio of NCP (11.4), and the fact that ASE and IC significantly modulate the C:N ratio further (Figure 6c), I conclude that the effect of lateral advection on larger scale integrals of the C:N ratio of NCP like those presented in this study (Table 3) can be ignored to the first order.

3.5.3. C:N Uptake Ratios From Changes in CO_2 and Nitrate

[35] Estimating the C:N ratio of new production from seasonal changes of nitrate and CO_2 implies that nitrate is the most significant source of new nitrogen in the system. Yet, little is known about the quantitative role of N_2 fixation in temperate and subpolar waters, in particular since direct measurements of N_2-fixation have focused on warm and oligotrophic waters [*Lipschultz and Owens*, 1996; *Capone et al.*, 1997]. Trichodesmium, the most conspicuous N_2 fixing genus, for example, usually grows in waters above 20°C [*Carpenter*, 1983]. A priori, there is no reason to exclude the possibility of N_2-fixation in temperate waters during summer, and, in fact, significant N_2 fixation has been reported, for example, from the Baltic Sea [*Wasmund et al.*, 2001]. However, conditions in the Baltic are specific in that

the nitrogen to phosphate ratios at the end of winter are much lower (7–8:1 [*Wasmund et al.*, 2001]), compared to the open Atlantic Ocean [*Koeve*, 2001] owing to denitrification in suboxic sediments of the Baltic [*Shaffer and Rönner*, 1984]. Phosphate concentrations of about 0.2 μmole kg^{-1} have been observed in the Baltic Proper when nitrate was depleted in early summer [*von Bodungen et al.*, 1981]. In the temperate and subpolar northeast Atlantic the winter time nitrate:phosphate ratio is very close to the Redfield value of 16 [*Koeve*, 2001] and phosphate depletes about the same time as nitrate [*Körtzinger et al.*, 2001a]. The magnitude of N_2-fixation required to explain the excess carbon production (equivalent to 0.2 mole N m^{-2} yr^{-1}) is huge compared with the amount of N_2-fixation suggested for tropical and subtropical waters (0.015 to 0.072 mole N m^{-2} yr^{-1} [*Orcutt et al.*, 2001; *Gruber and Sarmiento*, 1997] and hence should show up in the distribution of transient tracers in the interior of the ocean, namely the N* tracer [*Gruber and Sarmiento*, 1997], which is a measure of the excess NO_3 observed over the Redfield-equivalent of PO_4. However, compared to subtropical subsurface waters which show a strong positive N* signal and gradient indicating N_2-fixation, there is no comparable signal seen below temperate and subarctic waters [*Gruber and Sarmiento*, 1997, Figure 13]. Additionally, no evidence in the literature of direct N_2-fixation measurements [*Howarth et al.*, 1988; *Lipschultz and Owens*, 1996; *Capone et al.*, 1997] was found, which could question the a priori assumption of this paper that new production in temperate and subarctic waters is largely due to nitrate uptake. Hence it is concluded for the time being that new nitrogen production can be quantified in temperate and subarctic waters of the North Atlantic from a seasonal nitrate budget approach and that a C:N uptake ratio estimate based on seasonal budgets of NC_t and nitrate, like in this study, reflect the C:N ratio of NCP.

3.5.4. Seasonal Completeness of the Estimates

[36] New production is estimated in this study from the seasonal drawdown of nutrients and CO_2 between late winter and late summer. Hence it covers growth during spring and summer, but not during autumn. Little is known about the quantitative importance of the autumn phytoplankton bloom in the North Atlantic. From an analysis of the timing of minima and maxima in monthly averaged CZCS pigment data, *Campbell and Aarup* [1992] concluded that about 40% of the North Atlantic between 23°N and 70°N show a pigment peak during autumn. Overall, it appears from climatologies and model results [*Levitus*, 1982; *Woods and Barkmann*, 1986] that enhanced mixing, which is a necessary prerequisite of increased nutrient input to the euphotic zone and a possible autumn phytoplankton bloom, starts from September onward and is a slow process, in particular if compared with the rapid shallowing of the mixed layer observed during spring. This sluggishness is due to the fact that a large amount of heat, which accumulated during summer in the surface layer, has to be withdrawn from the Ocean before a significant mixed layer deepening and entrainment of new nutrients can take place. At the NABE-47 site, for example, the climatological mixed layer depth reaches about 70 m during November and the associated convective nitrate flux into the upper 30 m, which is the summer nitrate depleted layer at this site, is about 0.05 mole m^{-2} (computed from the NODC World Ocean Atlas 1998, not shown), which is equivalent to less than 10% of the spring + summer nitrate uptake in this region [*Koeve et al.*, 2002] (Figure 6a).

[37] The approach used in this paper is not capable of including autumn time new production in the seasonal budged. This is in particular due to the coarse horizontal, vertical and temporal resolution of nutrient and CO_2 data on the basin scale. *Lee* [2001] approached solving the underestimation issue by applying correction factors derived from the seasonal distribution of particulate carbon fluxes observed with sediment traps. For temperate and subarctic waters they assumed that autumn + winter carbon uptake is about 25% of spring + summer uptake. However, there is no simple means to translate such a correction factor sensitively to the C:N issue of this paper. Applying such a factor to both carbon and nitrate uptake estimates would not change the C:N uptake ratio. More importantly, a correction factor derived from the seasonal distribution of particle flux (export production) in seasonally dynamic systems cannot be applied to new production estimates without violating the steady state assumption, which is vital to the concept of the equality of new and export production [*Eppley and Peterson*, 1979], and its relevant timescales [*Platt et al.*, 1992]. In fact, the isotope signal of particles observed in deep traps of the northern North Atlantic [*Voss et al.*, 1996] indicates that ^{15}N-enriched particles arriving at depth (500 m) during autumn and winter are not derived from low ^{15}N-nitrate (new nitrogen), but are due to a slowly sinking particles stemming from the regenerated summer system. Particle fluxes observed late in the growth season are hence not an adequate means for the estimation of a correction factor to include autumn time NCP into an annual budget in temperate and subarctic waters. The example from the NABE 47°N site exemplifies that not accounting for autumn bloom new production in the estimates of the annual rate appears to be a minor problem, particularly for the C:N uptake ratio.

3.6. Seasonal Development of the C:N Ratio of New Production in the (Temperate) North Atlantic

[38] Our current knowledge of the C:N ratio of new production in the temperate and subarctic North Atlantic is based on short-term process studies (days to weeks [*Sambrotto et al.*, 1993a; *Kähler and Koeve*, 2001; *Koeve*, 2004]) and the analysis of data sets which cover variable parts of the growth season [*Körtzinger et al.*, 2001a]. None of these studies attempted to estimate the C:N ratio of new production over the whole growth season and on the basin scale. In this section I briefly discuss evidence from the published studies and relate it to findings from this paper.

[39] *Sambrotto et al.* [1993a] analyzed the temporal development of salinity normalized total CO_2 and nitrate data in the surface mixed layer observed during two drifting experiments in spring 1989 at the NABE-47°N site and found mean C:N ratios of new production of about 10 for the time period of a diatom bloom in late April to early May and larger than 9 (no ASE estimate available) during a flagellate bloom in late May [*Sieracki et al.*, 1993]. *Koeve* [2004] recently reanalyzed the same data set and found C:N

estimates to depend on a proper correction of preformed values; the respectively corrected short term averaged $(C:N)_{NCP}$ ratio during the diatom spring bloom was 7.3 ± 0.7.

[40] *Körtzinger et al.* [2001a] suggested that the C:N uptake ratio was close to or even below 6.6 during the phytoplankton spring bloom, increased at the end of the bloom and was significantly elevated in post-bloom waters at the southern boundary of the temperate northeast Atlantic. In that study nitrate and carbon based estimates of NCP were computed from winter time estimates (isopycnal outcrop analysis; see the data used in Figures 2 and 3), a midsummer transect from 30°N to 60°N along 20°W and an estimate of ASE similar to the one described in section 2.4. $CaCO_3$ formation was assumed to be an insignificant fraction of total CO_2 drawdown. A similar analysis of the cumulative C:N ratio of net community production for the 1989-NABE data from 47°N, 20°W gave an average integral spring bloom C:N ratio of 7.2 ± 0.9 [*Koeve*, 2004]. The approach used by *Körtzinger et al.* [2001a] and this study necessarily integrates over larger time and space scales, and, in the absence of N_2-fixation (see above), provides an estimate of the C:N ratio of NCP, $(C:N)_{NCP}$.

[41] C:N assimilation ratios of primary production, $(C:N)_{PP}$, can be computed from instantaneous isotope-based (^{15}N, ^{14}C) rate measurements of phytoplankton production. In systems where the f-ratio (NCP/PP) is high, the $(C:N)_{PP}$ may be taken as a first order proxy of $(C:N)_{NCP}$ simply since the majority of PP is NCP. During a process study at the NABE-47°N site $(C:N)_{PP}$ was close to Redfield, or lower, as long as nitrate was replete and the f-ratio was high [*Bury et al.*, 2001]. In a similar study of a late bloom situation in the northeast Atlantic at 58°N, 20°W (surface nitrate 1–2 μmole L^{-1}; surface chlorophyll *a* 1–1.2 μg L^{-1}; f-ratio = 0.8 ± 0.1 [*Boyd et al.*, 1997]), $(C:N)_{PP}$ ratios of 5.6 ± 2.3 (N = 8) were found. Both studies support the finding of *Körtzinger et al.* [2001a] and *Koeve* [2004] that excess carbon production is not related to the spring bloom but a feature of the summer system. The analysis from this study (Figure 8 and Table 3) that the late winter to late summer integrated $(C:N)_{NCP}$ ratio is elevated throughout the temperate and subarctic North Atlantic suggests that the finding of a seasonal progression of $(C:N)_{NCP}$ from low values in spring to high values in summer [*Körtzinger et al.*, 2001a] can be extended to the temperate and subarctic North Atlantic in general.

3.7. Source and Fate of Excess Carbon

[42] The presented evidence of elevated annual C:N ratios of net community production in large parts of the North Atlantic and the inferred finding that summertime carbon overconsumption is the most likely reason for the elevated spring + summer $(C:N)_{NCP}$ signal does not provide an a priori hint concerning the specific processes involved. Assuming that unrecognized N_2-fixation is an unlikely explanation (see section 3.5.2), both carbon overflow during primary production and subsequent exudation of carbon rich DOM [*Wood and Van Valen*, 1990] or preferential recycling of nitrogen over carbon [*Thomas et al.*, 1999] are possible source processes of carbon overconsumption. Whether the autotrophic pathway (carbon overflow) or the heterotrophic one (preferential recycling of N) dominates in the North Atlantic cannot be settled from the data presented in this study, but requires detailed in situ rate measurements. In either case, carbon rich (or nitrogen poor) material must be stored seasonally in the euphotic zone or become exported from the euphotic zone during summer in order to sustain a persistent $(C:N)_{NCP}$ until the end of summer. Seasonal storage of low-N dissolved organic carbon has been observed [*Williams*, 1995; *Kähler and Koeve*, 2001]; however, more data with an adequate seasonal coverage (including the wintertime start conditions) and from open ocean temperate or subarctic sites are needed to fully quantify the importance of this process in relation to the overall spring + summer $(C:N)_{NCP}$ ratios reported here. Seasonal storage of particulate organic material is unlikely to be important, since the C:N ratio of suspended POM is usually close to the Redfield value [*Copin-Montégut and Copin-Montégut*, 1983; *Körtzinger et al.*, 2001a] and since no significant amounts of POM accumulate during summer in the open ocean North Atlantic. Rapid export of excess carbon during summer via sinking particles appears unlikely if suspended particles have C:N ratios close to Redfield. DOM export during summer is limited due to the strong vertical density stratification.

[43] While DOM accumulation could not fully explain the spring to summer gradient in mixed layer $(C:N)_{NCP}$ and since the computed residual cumulative C:N ratio of exported matter showed a seasonal progression from spring into summer systems in the northeast Atlantic, *Körtzinger et al.* [2001a] speculated that TEP (transparent exopolymer particles [*Alldredge et al.*, 1993]) could be involved in export of excess carbon from the mixed layer. Extending this further, *Engel and Passow* [2001] and *Engel* [2002] have proposed that TEP, which has been shown to have a high C:N ratio [*Engel and Passow*, 2001; *Mari et al.*, 2001], may provide a vehicle by which carbon-rich DOM from carbon overconsumption in the euphotic zone interacts with sinking POM and hence contribute to particle export, even into the deep ocean. TEP, which probably form from polysaccharides released by phytoplankton and bacteria, is very surface-active and easily coagulate among themselves and with other particles [*Alldredge et al.*, 1993]. This reactivity gives rise to the mechanistic importance of TEP for particulate carbon fluxes in the ocean [*Passow*, 2002; *Boyd and Stevens*, 2002; *Passow*, 2004]. A non-Redfield "TEP-Pump" [*Koeve*, 2005] could provide a mechanism by which the total amount of carbon that is fixed in the ocean by phytoplankton and transported to the deep sea via the biological pump could well be more than calculated using the Redfield ratio [*Engel*, 2002].

[44] Evidence from particle flux studies provides constraints on the magnitude of the excess carbon export into the deep ocean. Studying a global data set of particle flux measurements, *Schneider et al.* [2003] concluded that the global mean C:N export ratio (Z = 100 m) is 7.1 ± 0.1 and that the average C:N ratio of sinking particles increases by about 0.2 ± 0.1 per 1000 m. Elevated C:N ratios of about 10 (or even up to 20) as frequently observed in the deep ocean, for example in freshly deposited detritus on the seafloor

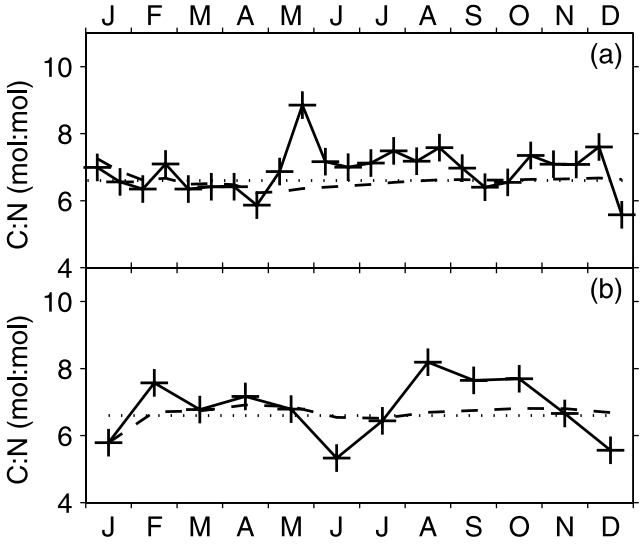

Figure 9. Annual cycles of C:N ratios of sinking particles in the North Atlantic. (a) Export production C:N ratios at the Bermuda Time Series Station BATS. Data from surface tethered particle interceptor traps deployed at 150 m between 1988 and 2001 (http://www.bbsr.edu/cintoo/bats/bats.html) are binned into 2-weekly intervals (crosses, solid line). (b) Carbon sequestration C:N ratios at the Biotrans Site (47°N, 20°W). Data from bottom moored particle interceptor traps deployed at 500 m between 1992 and 1996 (W. Koeve and B. Zeitzschel, unpublished data, 1996) were binned into monthly intervals (crosses, solid line). Dashed and dotted lines in both plots show the cumulative C:N ratio and the Redfield value of 6.6, respectively.

[*Smith et al.*, 1998; *Lampitt et al.*, 2001; *Beaulieu*, 2002], do not hold a valid information concerning C:N ratios of material exported from the euphotic zone since they are primarily caused by preferential remineralization of N over C [*Lee and Cronin*, 1984] during the decent of particles into the deep ocean [*Koeve*, 2005].

[45] Interseasonal differences of the C:N ratio of sinking particles have been reported repeatedly from deep ocean sediment traps in the North Atlantic [*von Bodungen et al.*, 1991; *Honjo and Manganini*, 1993]. At BATS, average C:N ratios of sinking particles in 150 m depth are around 7 during and after the spring bloom and increase to mean values around 8 during June to August (Figure 9a). In the temperate northeast Atlantic (47°N, 20°W) multiyear observations with moored sediment traps at 500 m depth show values around or below 7 during the spring bloom period (March to June) and values around 8 between August and October (Figure 9b). Both observations suggest that only a moderate fraction of the summertime carbon overconsumption appears to be exported from the euphotic zone (Figure 9a) or even sequestered below the winter mixed layer (Figure 9b).

[46] While direct export of dissolved organic matter is hindered during summer, it can be important during autumn when the stratification weakens and during winter when mixing reaches down to several hundred meters in the temperate and subarctic North Atlantic. Convective export of DOM out of the euphotic zone has been observed at the rim of the subtropical gyre [*Carlson et al.*, 1994; *Hansell and Carlson*, 2001], where the deepest mixing and the phytoplankton spring bloom co-occur. For the temperate Northeast Atlantic, where deep mixing and the spring bloom are mutually exclusive, only sporadic observations of convective DOM export from the euphotic zone are available (P. Kähler, personal communication, 2002) and its relative importance as a sink of excess carbon from the summer system can not be quantified by now.

[47] The finding (Figure 2b) that the a priori chosen AOU/nitrate remineralization ratio of −9.1 (equation (1)) yields winter nitrate concentrations that are in very good agreement with independent estimates, which do not apply any Redfield ratio assumption, suggests that the seasonal AOU on the plane of the climatological winter mixed layer depth is due to remineralization of carbon and nitrogen in Redfield proportion. This indicates that the spring + summer remineralization at this depth layer is mainly driven by freshly deposited material from the spring bloom, which is characterized by Redfield $(C:N)_{NCP}$ [*Körtzinger et al.*, 2001a; *Koeve*, 2004] as well as C:N ratios of export from the euphotic zone (Figure 9a) and C:N ratios of carbon sequestration (Figure 9b) close to the Redfield value. In turn this suggests that no significant (at least no detectable) amount of excess carbon reached the winter mixed layer plane, for example in the form of low-N DOM, by the end of summer. If, analogous to observations from the Pacific and Indian oceans [*Doval and Hansell*, 2000], no degradable DOC is subducted during the ventilation of mesopelagic waters at the end of winter, this may further point to limited deep export of excess carbon via low-N DOM during autumn and winter.

[48] If little excess carbon gets exported via particles (Figures 9a and 9b) [*Schneider et al.*, 2003; *Koeve*, 2005] or in the form of low-N DOM (last paragraph) what is the final sink of the excess carbon from summertime carbon overconsumption? One possibility, though yet to be tested by measurements, could be remineralization during autumn and early winter within a continuously deepening mixed layer. If this would be the dominant sink, lasting, that is export on timescales longer than one year, export of excess carbon might be small.

4. Summary and Conclusions

[49] The C:N ratio of net community production (NCP, new production, export production) in the temperate and subarctic North Atlantic is estimated from an analysis of winter and summer nitrate and salinity normalized total CO_2 (NC_t) data. Winter nitrate data are taken from climatologies [*Conkright et al.*, 1998; *Louanchi and Najjar*, 2000] and estimated from an extrapolation approach which maps the vertical nitrate distribution during summer into the seasonal development of nutrient concentrations at the sea surface [*Glover and Brewer*, 1988; *Koeve*, 2001]. From a comparison with springtime nitrate data and winter estimates from an isopycnal outcrop method, it is found that an improved

extrapolation technique which includes a correction for shallow seasonal remineralization of nitrate provides the most consistent estimate. The available climatological atlases do not capture the position of the N-S nutrient front in the North Atlantic. When NC_t is computed from empirical relationships with nitrate and temperature [*Lee et al.*, 2000], the uncertainties related to winter nitrate concentrations propagate and the initial uncertainties in winter NC_t estimates in the subarctic northeast Atlantic are of the same magnitude as the seasonal NC_t drawdown. However, when the winter NC_t is computed from the ''best choice'' winter nitrate data and SST, the NC_t distribution is found to be very much consistent with NC_t computed from winter alkalinity and pCO_2 and with winter NC_t estimates from an isopycnal outcrop estimate. Summer nitrate and NC_t data sets show much less variability between independent estimates and contribute comparatively little to the uncertainties in seasonal nitrate and NC_t uptake rates.

[50] Seasonal estimates of NCP during spring and summer are estimated from the seasonal drawdown of nitrate and NC_t in the upper 100 m, the CO_2 air-sea exchange and an estimate of the $CaCO_3$ production. For the temperate and subarctic North Atlantic between 40°N and 65°N an integral $(C:N)_{NCP}$ of 11.4 (±1.4) is estimated, where the error estimate includes random as well as systematic errors (wind speed dependence of air-sea exchange, overall OC:IC ratio).

[51] The analysis shown here extends the observation of significantly elevated $(C:N)_{NCP}$ for the integral spring + summer period from mesotrophic waters [*Körtzinger et al.*, 2001a] to the temperate and subarctic North Atlantic in general. Given that spring time $(C:N)_{NCP}$ ratios are close to the Redfield ratio [*Körtzinger et al.*, 2001a; *Koeve*, 2004], the excess biogenic carbon fixation appears to be due to net production during summer. Furthermore, assuming that the estimate of new nitrogen production is not an underestimate due to falsely neglecting N_2-fixation (see discussion in section 3.5.2) and that export of dissolved or particulate organic matter from the euphotic zone during summer provides only a limited sink of excess carbon (section 3.7), it is suggested that the seasonal storage of low-N DOM [*Williams*, 1995; *Kähler and Koeve*, 2001] is the likely dominant seasonal sink of most of the summertime carbon overconsumption. The ultimate fate of this material is yet unclear. Some may be exported laterally as low-N DOM during water mass subduction and some may become modified through the interaction between POC, DOC and TEP and sink to greater water depth. From the available evidence discussed in this paper, both processes appear to be subordinate. It is suggested that a large fraction may become remineralized during autumn and winter in the deepening mixed layer. Export of excess carbon below the winter mixed layer may therefore be small.

Appendix A: Statistical Error Analysis

[52] The uncertainty estimate of the basin scale integrated C:N ratio, $S_{(C:N)}$, is computed following equation (A1), which adopts the Gaussian error propagation procedure. Strictly speaking, this approach is valid for the propagation of standard deviations. However, in the lack of estimates of the standard deviations of the various terms needed to compute the C:N ratio, individual standard deviations are replaced by other uncertainty estimates. The final error estimate $S_{(C:N)}$ should not be mixed up with a formal estimate of the standard deviation of the basin-scale C:N ratio, it is rather a rough estimate of the uncertainty of this property. In A1 the terms ∂/∂ denote the partial differentials of equation (2) which are detailed in (A2) and (A3). Here ΔNO_3, ΔNC_t, ASE and ΔIC refer to the basin scale integrals of these properties.

$$S_{(C:N)} = \sqrt{\begin{aligned}&\left(\frac{\partial(C:N)}{\partial \Delta NCt}\right)^2 \cdot S^2_{\Delta NCt} + \left(\frac{\partial(C:N)}{\partial ASE}\right)^2 \cdot S^2_{ASE} \\ &+\left(\frac{\partial(C:N)}{\partial \Delta IC}\right)^2 \cdot S^2_{\Delta IC} + \left(\frac{\partial(C:N)}{\partial \Delta NO_3}\right)^2 \cdot S^2_{\Delta NO_3}\end{aligned}} \quad \text{(A1)}$$

$$\frac{\partial(C:N)}{\partial \Delta NCt} = \frac{\partial(C:N)}{\partial ASE} = \frac{\partial(C:N)}{\partial \Delta IC} = {}^{1}\Big/_{\Delta NO_3}, \quad \text{(A2)}$$

$$\frac{\partial(C:N)}{\partial \Delta NO_3} = -\frac{\Delta NC_t + ASE - \Delta IC}{(\Delta NO_3)^2}. \quad \text{(A3)}$$

[53] $S_{\Delta NCt}$, the uncertainty estimate of the integrated ΔNC_t is computed from the sum of the squares of local error estimates of ΔNC_t for each grid point (A4). The local error $s_{\Delta NCt}$ is calculated from (A5). Values for $s_{NCt(w)}$ and $s_{NCt(s)}$ are estimated as discussed in section 3.2 and 3.3 and are $s_{NCt(w)} = 6$ μmole kg^{-1} and $s_{NCt(s)} = 13$ μmole kg^{-1}. The latter value is the RMS difference between $T \times NO_3$ and $Alk \times pCO_2$ summer estimates. Equation (A5) is applied to the surface mixed layer and is transferred to the 100-m integral of ΔNC_t via the relative error ($s_{\Delta NCt}/\Delta NC_{t(ML)}$). For the computation of $S_{\Delta NO3}$ an analog treatment is carried out. Estimates of $s_{NO3(w)}$ and $s_{NO3(s)}$ are 0.5 μmole kg^{-1}.

$$\begin{aligned}S_{\Delta NCt} &= \sqrt{s^2_{\Delta NCt(i=1)} + s^2_{\Delta NCt(i=2)} + \ldots + s^2_{\Delta NCt(i=n)}} \\ &\approx \sqrt{n} \cdot s_{\Delta NCt}\end{aligned} \quad \text{(A4)}$$

$$s_{\Delta NCt} = \sqrt{s^2_{NC_{t(w)}} + s^2_{NC_{t(s)}}}. \quad \text{(A5)}$$

[54] For the air-sea CO_2 gas exchange the uncertainty is considerable [*Feely et al.*, 2001]. Namely uncertainties in the wind speed dependence of the gas transfer coefficient [*Liss and Merlivat*, 1986; *Wanninkhof*, 1992; *Nightingale et al.*, 2000] and in the accuracy of the monthly pCO_2 data set contribute to this uncertainty. I choose a local value of ±50% for the term $s_{ASE}/ASE*100$.

[55] The local uncertainty of the calcium carbonate production of the mixed layer, $s_{\Delta IC}$, is computed from (A6). The partial differentials ∂/∂ are given in (A7); $s_{\Delta NAt(ml)}$ and $s_{\Delta NO3(ml)}$ are computed in analogy to $s_{\Delta NCt(ml)}$ (see above). Estimates for $s_{NAt(w)}$ and $s_{NAt(s)}$ of 5 μmole kg^{-1} are taken from the analysis of *Millero et al.* [1998]. It is assumed that

the local relative error of the surface mixed layer and of the 100-m integral of calcium carbonate production are the same. The integral uncertainty estimate of the basin scale estimate of ΔIC, $S_{\Delta IC}$, is computed from the distribution of $s_{\Delta IC}$ in analogy to equation (A4).

$$s_{\Delta IC(ml)} = \sqrt{\left(\frac{\partial \Delta IC_{(ml)}}{\partial \Delta NA_{t_{(ml)}}}\right)^2 \cdot s^2_{\Delta NA_{t(ml)}} + \left(\frac{\partial \Delta IC_{(ml)}}{\partial \Delta NO_{3_{(ml)}}}\right)^2 \cdot s^2_{\Delta NO_{3(ml)}}} \quad \text{(A6)}$$

$$\frac{\partial \Delta IC_{(ml)}}{\partial \Delta NA_{t(ml)}} = \frac{\partial \Delta IC_{(ml)}}{\partial \Delta NO_{3(ml)}} = {}^1\!/_2. \quad \text{(A7)}$$

[56] Typical values for the local errors, here given for the JGOFS-NABE 47°N site, for the KexWOAmin data set are as follows: 23% ($s_{\Delta NCt(rel)}$), 10% ($s_{\Delta NO3(rel)}$), 30% ($s_{\Delta IC(rel)}$) and 50% ($s_{ASE(rel)}$). Through the process of lateral integration local errors are propagated like shown in equation (A4). The integration involves 1461 grid points between 40°N and 65°N. If all grid points would have the same property values, the relative errors for property x would scale as $S_{x(rel)}/s_{x(rel)} = \sqrt{n}/n = 0.026$. In fact integral uncertainties roughly follow this prediction: 0.9% ($S_{\Delta NCt(rel)}$), 0.4% ($S_{\Delta NO3(rel)}$), 1% ($S_{\Delta IC(rel)}$), 1.5% ($S_{ASE(rel)}$). The combined error of the estimate of the integral C:N ratio is 0.11.

[57] This is a too optimistic estimate of the error since it depends on the arbitrarily chosen resolution of the horizontal grid. The number of grid point for which data are available is much lower and variable for different data sets. For example the WOA summer nitrate data set has 392 and the WOA98 annual nitrate data sets, on which KexNO3 builds, 532 significant grid points between 40°N and 65°N. The respective $S_{x(rel)}/s_{x(rel)}$ scaling factors are 0.05 and 0.043. I correct the integrated relative errors ($S_{\Delta NCt(rel)}$, etc.) by applying the ratio 0.05/0.026. The statistical error of the integral C:N ratio estimate is 0.16. Systematic errors, for example due to uncertainties in the wind speed dependence of CO_2 air-sea exchange, or the overall OC:IC ratio are about 1 order of magnitude larger and are discussed in section 3.5.1.

[58] **Acknowledgments.** Thanks are owed to T. Takahashi and his group for providing the pCO_2 air-sea difference data set used in this study. The author wishes to acknowledge use of the Ferret program for data analysis in this paper. Ferret (http://www.ferret.noaa.gov) is a product of NOAA's Pacific Marine Environmental Laboratory. This work was supported by the German JGOFS synthesis program via a grant of the German BMB+F to G. Wefer and W. Koeve and by the French CNRS via a poste rouge grant to V. Garçon and W. Koeve. Comments by Ray Sambrotto and one anonymous reviewer helped to clarify the ideas and the presentation.

References

Abell, J., S. Emerson, and P. Renaud (2000), Distribution of TOP, TON, TOC in the North Pacific subtropical gyre: Implications for nutrient supply in the surface ocean and remineralization in the upper thermocline, *J. Mar. Res.*, *58*, 203–222.

Alldredge, A. L., U. Passow, and B. E. Logan (1993), The abundance and significance of a class of large, transparent organic particles in the ocean, *Deep Sea Res., Part I*, *40*, 1131–1140.

Anderson, L. A. (1995), On the hydrogen and oxygen content of marine phytoplankton, *Deep Sea Res., Part I*, *42*, 1675–1680.

Anderson, L. A., and J. L. Sarmiento (1994), Redfield ratios of remineralization determined by nutrient data analysis, *Global Biogeochem. Cycles*, *8*, 65–80.

Antonov, J., S. Levitus, T. P. Boyer, M. Conkright, T. O'Brien, and C. Stephens (1998), *World Ocean Atlas 1998*, vol. 1, *Temperature of the Atlantic Ocean*, *NOAA Atlas NESDIS 27*, 166 pp., NOAA, Silver Spring, Md.

Bates, N. R., A. F. Michaels, and A. H. Knap (1996), Seasonal and interannual variability of oceanic carbon dioxide species at the U.S. JGOFS Bermuda Atlantic Times-series Station (BATS) site, *Deep Sea Res., Part II*, *43*, 347–383.

Beaulieu, S. (2002), Accumulation and fate of phytodetritus on the sea floor, *Oceanogr. Mar. Biol.*, *40*, 171–232.

Boyd, P. W., and C. L. Stevens (2002), Modelling particle transformations and the downward organic carbon flux in the NE Atlantic Ocean, *Prog. Oceanogr.*, *52*, 1–29.

Boyd, P., A. Pomroy, S. Bury, G. Savidge, and I. Joint (1997), Microalgal carbon and nitrogen uptake in post-coccolithophore bloom conditions in the northeast Atlantic, July 1991, *Deep Sea Res., Part I*, *44*, 1497–1517.

Boyer, T., M. E. Conkright, and S. Levitus (1999), Seasonal variability of dissolved oxygen, percent oxygen saturation, and apparent oxygen utilization in the Atlantic and Pacific Oceans, *Deep Sea Res., Part I*, *46*, 1593–1613.

Brewer, P. G., J. L. Sarmiento, and W. M. Smethie (1985), The transient tracers in the ocean (TTO) program: The North Atlantic study, 1981; the Tropical Atlantic study, 1983, *J. Geophys. Res.*, *90*, 6903–6905.

Bury, S. J., P. W. Boyd, T. Preston, T. Savidge, G. Savidge, and N. J. P. Owens (2001), Size-fractionated primary production and nitrogen uptake during a North Atlantic phytoplankton bloom: Implications for carbon export estimates, *Deep Sea Res., Part I*, *48*, 689–720.

Campbell, J. W., and T. Aarup (1992), New production in the North Atlantic derived from seasonal patterns of surface chlorophyll, *Deep Sea Res.*, *39*, 1669–1694.

Capone, D. G., J. P. Zehr, H. W. Paerl, B. Bergman, and E. J. Carpenter (1997), Trichodesmium, a globally significant marine cyanobacterium, *Science*, *276*, 1221–1229.

Carlson, C. A., H. W. Ducklow, and A. F. Michaels (1994), Annual flux of dissolved organic carbon from the euphotic zone in the northwestern Sargasso Sea, *Nature*, *371*, 405–408.

Carpenter, E. J. (1983), Nitrogen fixation by marine Oscillatoria (Trichodesmium) in the Word's Ocean, in *Nitrogen in the Marine Environment*, edited by E. J. Carpenter and D. G. Capone, pp. 65–104, Elsevier, New York.

Codispoti, L. A. (1997), The limits of growth, *Nature*, *387*, 237–238.

Conkright, M., T. O'Brien, S. Levitus, T. P. Boyer, J. Antonov, and C. Stephens (1998), *World Ocean Atlas 1998*, vol. 10, *Nutrients and Chlorophyll of the Atlantic Ocean*, *NOAA Atlas NESDIS 36*, 245 pp., NOAA, Silver Spring, Md.

Copin-Montégut, C., and G. Copin-Montégut (1983), Stoichiometry of carbon, nitrogen, and phosphorus in marine particulate matter, *Deep Sea Res.*, *30*, 31–46.

Craig, H., and T. Hayward (1987), Oxygen supersaturation in the ocean: Biological versus physical contributions, *Science*, *235*, 199–202.

Daly, K., D. Wallace, O. J. Smith, R. Skoog, M. Gosselin, E. Falck, and P. Yager (1999), Non-Redfield carbon and nitrogen cycling in the Arctic: Effects of ecosystem structure and dynamics, *J. Geophys. Res.*, *104*, 3185–3199.

Dickson, A. G., and F. J. Millero (1987), A comparison of the equilibrium constants for the dissociation of carbonic acid in seawater media, *Deep Sea Res.*, *36*, 1733–1743.

Doval, M. D., and D. A. Hansell (2000), Organic carbon and apparent oxygen utilization in the western South Pacific and the central Indian Ocean, *Mar. Chem.*, *68*, 249–264.

Ducklow, H. W., and R. P. Harris (1993), JGOFS: The North Atlantic Bloom Experiment, *Deep Sea Res., Part II*, *40*, 1–641.

Dugdale, R. C., and J. J. Goering (1967), Uptake of new and regenerated forms of nitrogen in primary productivity, *Limnol. Oceanogr.*, *12*, 196–206.

Emerson, S., and T. L. Hayward (1995), Chemical tracers of biological processes in shallow waters of North Pacific: Preformed nitrate distribution, *J. Mar. Res.*, *53*, 499–513.

Emerson, S., P. Quay, C. Stump, D. Wilbur, and R. Schudlich (1993), Determining primary production from the mesoscale oxygen field, *ICES Mar. Sci. Symp.*, *197*, 196–206.

Emerson, S., P. Quay, D. Karl, C. Winn, L. Tupas, and M. Landry (1997), Experimental determination of the organic carbon flux from the open-ocean surface waters, *Nature*, *389*, 951–954.

Engel, A. (2002), Direct relationship between CO_2 uptake and transparent exopolymer particles production in natural phytoplankton, *J. Plankton Res.*, *24*, 49–53.

Engel, A., and U. Passow (2001), Carbon and nitrogen content of transparent exopolymer particles (TEP) in relation to their Alcian Blue adsorption, *Mar. Ecol. Prog. Ser.*, *219*, 1–10.

Eppley, R. W., and B. J. Peterson (1979), Particulate organic matter flux and planktonic new production in the deep ocean, *Nature*, *282*, 677–680.

Esbensen, S. K., and Y. Kushnir (1981), The heat budget of the global ocean: An atlas based on estimates from surface marine observations, *Tech Rep. 29*, Clim. Res. Inst., Oreg. State Univ., Corvallis.

Fasham, M. J. R., B. M. Balino, and M. C. Bowles (2001), A new vision of ocean biogeochemistry after a decade of the Joint Global Ocean Flux Study (JGOFS), *Ambio*, *10*, 4–30.

Feely, R. A., C. L. Sabine, T. Takahashi, and R. Wanninkhof (2001), Uptake an storage of carbon dioxide in the ocean: The global CO_2 survey, *Oceanography*, *14*, 18–32.

Fiadeiro, M. (1980), The alkalinity of the deep pacific, *Earth Planet. Sci. Lett.*, *49*, 499–505.

Glover, D. M., and P. G. Brewer (1988), Estimates of wintertime mixed layer nutrient concentration in the North Atlantic, *Deep Sea Res.*, *35*, 1525–1546.

Gruber, N., and J. L. Sarmiento (1997), Global patterns of marine nitrogen fixation and denitrification, *Global Biogeochem. Cycles*, *11*, 235–266.

Hansell, D. A., and C. A. Carlson (2001), Biogeochemistry of total organic carbon and nitrogen in the Sargasso Sea: Control by convective overturn, *Deep Sea Res., Part II*, *48*, 1649–1667.

Hedges, J. I., J. A. Baldock, Y. Gélinas, C. Lee, M. L. Peterson, and S. G. Wakeham (2002), The biogeochemical and elemental composition of marine plankton: A NMR perspective, *Mar. Chem.*, *78*, 47–63.

Honjo, S., and S. J. Manganini (1993), Annual biogenic particle fluxes to the interior of the North Atlantic Ocean, studied at 34°N 21°W and 48°N 21°W, *Deep Sea Res., Part II*, *40*, 587–608.

Howarth, R. W., R. Marino, J. Lane, and J. J. Cole (1988), Nitrogen fixation in freshwater, estuarine, and marine ecosystems: 1. Rates and importance, *Limnol. Oceanogr.*, *33*, 669–687.

Jenkins, W. J., and J. C. Goldman (1985), Seasonal oxygen cycling and primary production in the Sargasso Sea, *J. Mar. Res.*, *43*, 465–491.

Kähler, P., and W. Koeve (2001), Marine dissolved organic matter: Can its C/N ratio explain carbon overconsumption?, *Deep Sea Res., Part I*, *48*, 49–62.

Kalnay, E., et al. (1996), The NCEP/NCAR 40-year reanalysis project, *Bull. Am. Meteorol. Soc.*, *77*, 437–471.

Koeve, W. (2001), Wintertime nutrients in the North Atlantic—New approaches and implications for estimates of seasonal new production, *Mar. Chem.*, *74*, 245–260.

Koeve, W. (2002), Upper ocean carbon fluxes in the Atlantic Ocean: The importance of the POC:PIC ration, *Global Biogeochem. Cycles*, *16*(4), 1056, doi:10.1029/2001GB001836.

Koeve, W. (2004), Spring bloom carbon to nitrogen ratio of net community production in the temperate N. Atlantic, *Deep Sea Res., Part I*, *51*, 1579–1600.

Koeve, W. (2005), Magnitude of excess carbon sequestration into the deep ocean and the possible role of TEP, *Mar. Ecol. Prog. Ser.*, *291*, 53–64.

Koeve, W., and H. Ducklow (2001), JGOFS synthesis and modelling: The North Atlantic ocean, *Deep Sea Res., Part II*, *48*, 2141–2154.

Koeve, W., F. Pollehne, A. Oschlies, and B. Zeitzschel (2002), Storm induced convective export of organic matter during spring in the northeast Atlantic, *Deep Sea Res., Part I*, *49*, 1431–1444.

Körtzinger, A., W. Koeve, P. Kähler, and L. Mintrop (2001a), C:N ratios in the mixed layer during the productive season in the northeast Atlantic ocean, *Deep Sea Res., Part I*, *48*, 661–688.

Körtzinger, A., J. I. Hedges, and P. D. Quay (2001b), Redfield ratios revisited—Removing the biasing effect of anthropogenic CO_2, *Limnol. Oceanogr.*, *46*, 964–970.

Lampitt, R. S., B. J. Bett, K. Kiriakoulakis, E. E. Popova, O. Ragueneau, A. Vangriesheim, and G. A. Wolff (2001), Material supply to the abyssal seafloor in the Northeast Atlantic, *Prog. Oceanogr.*, *50*, 27–63.

Lee, C., and C. Cronin (1984), Particulate amino acids in the sea: Effects of primary productivity and biological decomposition, *J. Mar. Res.*, *42*, 1075–1097.

Lee, K. (2001), Global net community production estimated from the annual cycle of surface water total dissolved inorganic carbon, *Limnol. Oceanogr.*, *46*, 1287–1297.

Lee, K., F. J. Millero, and R. Wanninkhof (1997), The carbon dioxide system in the Atlantic Ocean, *J. Geophys. Res.*, *102*, 15,693–15,707.

Lee, K., R. H. Wanninkhof, R. A. Feely, F. J. Millero, and T.-H. Peng (2000), Global relationships of total inorganic carbon with temperature and nitrate in surface water, *Global Biogeochem. Cycles*, *14*, 979–994.

Levitus, S. (1982), Climatological atlas of the world ocean, *NOAA Prof. Pap. 13*, pp. 1–41, U.S. Gov. Print. Off., Washington, D. C.

Lewis, E., and D. W. R. Wallace (1998), Program developed for CO_2 system calculations, *Rep. ORNL/CDIAC-105*, Carbon Dioxide Inf. Anal. Cent., Oak Ridge Natl. Lab., Oak Ridge, Tenn.

Li, Y. H., and T. H. Peng (2002), Latitudinal change of the remineralization ratios in the oceans and its implication for nutrient cycles, *Global Biogeochem. Cycles*, *16*(4), 1130, doi:10.1029/2001GB001828.

Lipschultz, F., and N. J. P. Owens (1996), An assessment of nitrogen fixation as a source of nitrogen to the North Atlantic Ocean, *Biogeochemistry*, *35*, 261–274.

Lipschultz, F., N. R. Bates, C. A. Carlson, and D. A. Hansell (2002), New production in the Sargasso Sea: History and current status, *Global Biogeochem. Cycles*, *16*(1), 1001, doi:10.1029/2000GB001319.

Liss, P. S., and L. Merlivat (1986), Air-sea gas exchange rates: Introduction and synthesis, in *The Role of Air-Sea Exchange in Geochemical Cycling*, edited by P. Buat-Ménard, pp. 113–127, Springer, New York.

Louanchi, F., and R. G. Najjar (2000), A global monthly climatology of phosphate, nitrate and silicate in the upper ocean: Spring-summer export production and shallow remineralization, *Global Biogeochem. Cycles*, *14*, 957–977.

Mari, X., S. Beauvais, R. Lemee, and M. Pedrotti (2001), Non-Redfield C:N ratio of transparent exopolymeric particles in the northwestern Mediterranean Sea, *Limnol. Oceanogr.*, *46*, 1831–1836.

Masarie, K. A., and P. P. Tans (1995), Extension and integration of atmospheric carbon dioxide data into a globally consistent measurement record, *J. Geophys. Res.*, *100*, 11,593–11,610.

Mehrbach, C., C. H. Culberson, J. E. Hawley, and R. M. Pytkowicz (1973), Measurement of the apparent dissociation constants of carbonic acid in seawater at atmospheric pressure, *Limnol. Oceanogr.*, *18*, 897–907.

Millero, F. J., K. Lee, and M. Roche (1998), Distribution of alkalinity in the surface waters of the major oceans, *Mar. Chem.*, *60*, 111–130.

Minas, H. J., and L. A. Codispoti (1993), Estimates of primary production by observation of changes in the mesoscale nitrate field, *ICES Mar. Sci. Symp.*, *197*, 215–235.

Minster, J.-F., and M. Boulahdid (1987), Redfield ratios along isopycnal surfaces—A complementary study, *Deep Sea Res.*, *34*, 1981–2003.

Monterey, G., and S. Levitus (1997), *Seasonal Variability of Mixed Layer Depth for the World Ocean*, *NOAA Atlas NESDIS 14*, 96 pp., NOAA, Silver Spring, Md.

Najjar, R. G., and R. F. Keeling (2000), Mean annual cycle of the air-sea oxygen flux: A global view, *Global Biogeochem. Cycles*, *14*, 573–584.

Nightingale, P. D., G. Malin, C. S. Law, A. J. Watson, P. S. Liss, M. I. Lidicoat, J. Boutin, and R. C. Upstill-Godard (2000), In situ evaluation of air-sea gas exchange parameterizations using novel conservative and volatile tracers, *Global Biogeochem. Cycles*, *14*, 373–387.

Ono, S., A. Ennyu, R. G. Najjar, and N. R. Bates (2001), Shallow remineralization in the Sargasso Sea estimated from seasonal variations in oxygen, dissolved inorganic carbon and nitrogen, *Deep Sea Res., Part II*, *48*, 1567–1582.

Orcutt, K. M., F. Lipschultz, K. Gundersen, R. Arimoto, A. F. Michaels, A. H. Knap, and J. R. Gallon (2001), A seasonal study of the significance of N_2 fixation by Trichodesmium spp. at the Bermuda Atlantic time-series study (BATS) site, *Deep Sea Res., Part II*, *48*, 1583–1608.

Oschlies, A., W. Koeve, and V. Garçon (2000), An eddy-permitting coupled physical-biological model of the North Atlantic: 2. Ecosystem dynamics and comparison with satellite and JGOFS local studies data, *Global Biogeochem. Cycles*, *14*, 499–523.

Passow, U. (2002), Transparent exopolymer particles (TEP) in aquatic environments, *Prog. Oceanogr.*, *55*, 287–333.

Passow, U. (2004), Switching perspectives: Do mineral fluxes determine particulate organic carbon fluxes or vice versa?, *Geochem. Geophys. Geosyst.*, *5*, Q04002, doi:10.1029/2003GC000670.

Platt, T., P. Jauhari, and S. Sathyendranath (1992), The importance and measurement of new production, in *Primary Productivity and Biogeochemical Cycles in the Sea*, edited by P. G. Falkowski and A. D. Woohead, pp. 273–284, Springer, New York.

Redfield, A. C., B. H. Ketchum, and F. A. Richards (1963), The influence of organisms on the composition of seawater, in *The Sea*, vol. 2, edited by M. N. Hill, pp. 26–77, John Wiley, Hoboken, N. J.

Robertson, J. E., C. Robinson, D. R. Turner, P. Holligan, A. J. Watson, P. Boyd, E. Fernandez, and M. Finch (1994), The impact of a coccolithophore bloom on oceanic carbon uptake in the northeast Atlantic during summer 1991, *Deep Sea Res., Part I*, *41*, 297–314.

Sambrotto, R. N., G. Savidge, C. Robinson, P. Boyd, T. Takahashi, D. M. Karl, C. Langdon, D. Chipman, J. Marra, and L. Codispoti (1993a), Elevated consumption of carbon relative to nitrogen in the surface ocean, *Nature*, *363*, 248–250.

Sambrotto, R. N., J. H. Martin, W. W. Broenkow, C. Carlson, and S. E. Fitzwater (1993b), Nitrate utilization in surface waters of the Iceland Basin during spring and summer of 1989, *Deep Sea Res., Part II*, *40*, 441–458.

Sarmiento, J. L., J. Dunne, A. Gnanadesikan, R. M. Key, K. Matsumoto, and R. Slater (2002), A new estimate of the $CaCO_3$ to organic carbon export ratio, *Global Biogeochem. Cycles*, *16*(4), 1107, doi:10.1029/2002GB001919.

Schlitzer, R. (2000), Electronic atlas of WOCE hydrographic and tracer data now available, *Eos Trans. AGU*, *81*, 45.

Schneider, B., R. Schlitzer, G. Fischer, and E.-M. Nöthig (2003), Depth-dependent elemental compositions of particulate organic matter (POM) in the ocean, *Global Biogeochem. Cycles*, *17*(2), 1032, doi:10.1029/2002GB001871.

Scientific Committee on Oceanic Research (1990), The Joint Global Ocean Flux Study—JGOFS Science Plan, report, 61 pp., Int. Counc. of Sci. Unions, Halifax, N. S., Canada.

Shaffer, G. (1993), Effects of the marine biota on global carbon cycling, in *The Global Carbon Cycle*, edited by M. Heimann, pp. 431–455, Springer, New York.

Shaffer, G. (1996), Biogeochemical cycling in the global ocean: 2. New production, Redfield ratios, and remineralization in the organic pump, *J. Geophys. Res.*, *101*, 3723–3745.

Shaffer, G., and U. Rönner (1984), Denitrification in the Baltic proper deep water, *Deep Sea Res.*, *31*, 197–220.

Sieracki, M., P. G. Verity, and D. K. Stoecker (1993), Plankton community response to sequential silicate and nitrate depletion during the 1989 North Atlantic spring bloom, *Deep Sea Res., Part II*, *40*, 213–226.

Smith, K. L. J., R. J. Baldwin, R. C. Glatts, R. S. Kaufmann, and E. C. Fisher (1998), Detrital aggregates on the sea floor: Chemical composition and aerobic decomposition rates at a time-series station in the abyssal NE Pacific, *Deep Sea Res., Part II*, *45*, 843–880.

Strass, V., and J. D. Woods (1988), Horizontal and seasonal variations of density and chlorophyll profiles between the Azores and Greenland, in *Towards a Theory of Biological-Physical Interactions in the World Ocean*, edited by B. J. Rothchild, pp. 113–136, Springer, New York.

Strass, V. H., and J. D. Woods (1991), New production in the summer revealed by the meridional slope of the deep chlorophyll maximum, *Deep Sea Res.*, *38*, 35–56.

Takahashi, T., W. S. Broecker, and S. Langer (1985), Redfield ratio based on chemical data from isopycnal surfaces, *J. Geophys. Res.*, *90*, 6907–6924.

Takahashi, T., J. Olafsson, J. G. Goddard, D. W. Chipman, and S. C. Sutherland (1993), Seasonal variation of CO_2 and nutrients in the high-latitude surface ocean: A comparative study, *Global. Biogeochem. Cycles*, *7*, 843–878.

Takahashi, T., R. H. Wanninkhof, R. A. Feely, R. F. Weiss, D. W. Chipman, N. Bates, J. Olafsson, C. Sabine, and S. C. Sutherland (1999), Net sea-air CO_2 flux over the global oceans: An improved estimate based on the sea-air pCO_2 difference, in *Proceedings of the 2nd International Symposium CO_2 in the Oceans, Tsukuba, January 1999, CGER-1037-'99*, pp. 9–15, Cent. for Global Environ. Res., Tsukuba, Japan.

Thomas, H., V. Ittekkot, C. Osterroht, and B. Schneider (1999), Preferential recycling of nutrients—The ocean's way to increase new production and to pass nutrient limitation, *Limnol. Oceanogr.*, *44*, 1999–2004.

von Bodungen, B., K. von Bröckel, V. Smetacek, and B. Zeitzschel (1981), Growth and sedimentation of the phytoplankton spring bloom in the Bornholm Sea (Baltic Sea), *Kiel. Meeresforsch, Sonderh.*, *5*, 49–60.

von Bodungen, B., U. Bathmann, M. Voss, and M. Wunsch (1991), Vertical particle flux in the Norwegian Sea—Resuspension and interannual variability, in *Sediment Trap Studies in the Nordic Countries*, vol. 2, *Proceedings*, edited by P. Wassmann, A.-S. Heiskanen, and O. Lindahl, pp. 116–136, Nurmiprint OY, Nurmijärvi, Finland.

Veldhuis, M. J. W., G. W. Kraay, and W. W. C. Gieskes (1993), Growth and fluorescence characteristics of ultraplankton on a north-south transect in the eastern North Atlantic, *Deep Sea Res., Part II*, *40*, 609–626.

Volk, T., and M. I. Hoffert (1985), Ocean carbon pumps, analysis of relative strengths and efficiencies in ocean-driven atmosphereCO_2 changes, in *The Carbon Cycle and Atmospheric CO_2: Natural Variations Archean to Present*, *Geophys. Monogr. Ser.*, vol. 32, edited by E. T. Sundquist and W. S. Broecker, pp. 99–110, AGU, Washington, D. C.

Voss, M., M. A. Altabet, and B. von Bodungen (1996), $\delta^{15}N$ in sedimenting particles as indicator of euphotic-zone processes, *Deep Sea Res.*, *43*, 33–47.

Wanninkhof, R. (1992), Relationship between wind speed and gas exchange over the ocean, *J. Geophys. Res.*, *97*, 7373–7382.

Wanninkhof, R., and W. M. McGillis (1999), A cubic relationship between gas transfer and wind speed, *Geophys. Res. Lett.*, *26*, 1889–1893.

Wasmund, N., M. Voss, and K. Lochte (2001), Evidence of nitrogen fixation by non-heterocystous cyanobacteria in the Baltic Sea and re-calculation of a budget of nitrogen fixation, *Mar. Ecol. Prog. Ser.*, *214*, 1–14.

Weiss, R. W. (1974), Carbon dioxide in water and seawater: The solubility of a non-ideal gas, *Mar. Chem.*, *2*, 203–215.

Williams, P. J. L. B. (1995), Evidence for the seasonal accumulation of carbon-rich dissolved organic material, its scale in comparison with changes in particulate material and the consequential effect on net C/N assimilation ratios, *Mar. Chem.*, *51*, 17–29.

Wood, A. M., and L. M. Van Valen (1990), Paradox lost? On the release of energy-rich compounds by phytoplankton, *Mar. Microb. Food Webs*, *4*, 103–116.

Woods, J. D., and W. Barkmann (1986), The response of the upper ocean to solar heating: I. The mixed layer, *Q. J. R. Meteorol. Soc.*, *112*, 1–27.

Yentsch, C. S. (1990), Estimates of new production in the mid-North Atlantic, *J. Plankton Res.*, *12*, 717–734.

W. Koeve, Leibniz-Institut für Meereswissenschaften (IFM-GEOMAR), Dienstgebäude Westufer, Düsternbrooker Weg 20, D-24105 Kiel, Germany. (w.koeve@web.de)